NASA TECHNICAL NOTE

NASA TN D-2066

NASA TN D-2066

EVALUATION OF A CONSTRICTED-ARC SUPERSONIC JET

by Charles E. Shepard, Velvin R. Watson, and Howard A. Stine

Ames Research Center
Moffett Field, California

NATIONAL AERONAUTICS AND SPACE ADMINISTRATION • WASHINGTON, D. C. • JANUARY 1964

EVALUATION OF A CONSTRICTED-ARC SUPERSONIC JET

By Charles E. Shepard, Velvin R. Watson,
and Howard A. Stine

Ames Research Center
Moffett Field, Calif.

NATIONAL AERONAUTICS AND SPACE ADMINISTRATION

For sale by the Office of Technical Services, Department of Commerce,
Washington, D.C. 20230 -- Price $1.00

EVALUATION OF A CONSTRICTED-ARC SUPERSONIC JET

By Charles E. Shepard, Velvin R. Watson,
and Howard A. Stine

SUMMARY

A constricted-arc supersonic jet has been constructed and tested. An electric arc originates in the plenum chamber and is passed completely through the supersonic nozzle into the test section. The arc is maintained through the nozzle without disrupting the supersonic flow. High total enthalpies are produced by forcing the gas to flow through the arc column within an elongated, well-cooled throat that acts to thermally constrict the discharge.

The throat, or constrictor tube, was 1/4 inch in diameter and approximately 3 inches long. Performance was determined for a range of currents from 108 to 240 amperes and nitrogen flow rates from 3.1×10^{-4} to 11.5×10^{-4} lb/sec. Average total enthalpies were determined by means of a balance between the electrical power supplied to the gas stream and the power losses to the various water-cooled components. Average enthalpies in excess of 30,000 Btu/lb were measured in the gas at the downstream end of the constrictor tube.

The heating of the gas in the constant-area section of the nozzle was studied in detail. Laminar conduction was the predominant heat loss mechanism from the gas to the water-cooled constrictor walls. The experimental results were compared with an analysis by Stine and Watson of an arc column with laminar conduction heat losses. It was found that the analysis predicted all important trends in the experimental data.

INTRODUCTION

In conventional plasma jets, such as the one shown conceptually in figure 1, the working fluid is heated at constant pressure in an arc chamber before being passed through a supersonic nozzle. Although in a suitably arranged arc chamber the gas within the arc column can attain high enthalpy, subsequent losses to the walls of the plenum chamber and the nozzle appear to limit the maximum enthalpy available in the test section to about 15,000 Btu/lb in air or nitrogen (ref. 1).

In the constricted-arc supersonic jet reported herein, an electric arc originating in the plenum chamber is passed completely through the supersonic nozzle and into the test section (fig. 2). Enthalpies in excess of 30,000 Btu/lb are produced by forcing the gas to flow through the arc column within an elongated throat that acts to thermally constrict the discharge.

Although "wall constricted" arcs are known to generate high enthalpy in a static gas, and have been studied for many years (refs. 2 and 3), a high-enthalpy supersonic jet is difficult to achieve by merely locating the constrictor within the arc chamber upstream of the aerodynamic throat. The heated gas cools very

rapidly, and large losses appear in the plenum chamber and the nozzle. In the device shown in figure 2, however, the constrictor is also the aerodynamic throat. In addition, the power available to the gas throughout the expanding portion of the nozzle compensates for the large heat losses, and the enthalpy achieved within the throat is maintained throughout the expanding portion and becomes available in the test section.

The throat region shown in figure 2 is longer than is desirable from a purely aerodynamic standpoint, but provides a cylindrical constrictor tube wherein the enthalpy can achieve high values with reasonably low values of arc current. The rate of enthalpy rise is greatest at the beginning of the throat region, where the gas is coldest and the electrical resistance is the greatest. At some distance along the tube, depending on the mass flow, the rate of increase approaches zero, and the enthalpy tends to an asymptotic value. If the flow is laminar, and if radiation is unimportant, the heating process in the cylindrical constrictor is amenable to analysis (ref. 4), and the rate of enthalpy rise can be calculated.

The purposes of this report are threefold: First, a description of the components of the constricted-arc supersonic jet and a rationale for design will be presented. Second, data consisting of detailed measurements of the heat loss and voltage distributions along the constrictor will be discussed. Third, various predictions of the laminar theory will be compared with the experimental results.

SYMBOLS

A	parameter of the approximation $\sigma = A\varphi$ used in reference 4, mho-sec/Btu
A^*	nozzle throat area, ft^2
c_p	specific heat at constant pressure, Btu/lb $^\circ F$
D	diameter
E	voltage gradient, volt/ft
H	mass average enthalpy, Btu/lb (reference value is 0 at 530° R)
H_E	radially averaged enthalpy, Btu/lb (reference value is 0 at 530° R)
I	current, amp
k	thermal conductivity, Btu/ft $^\circ R$ sec
P	power loss, Btu/sec
p	pressure, atm

p_o plenum chamber pressure, atm

q heat flux, Btu/ft^2 sec

r_e radius of the current-carrying cylinder, ft

r_w radius of constrictor tube, ft

T temperature, ^oR

V voltage, volts

$\dot{w}$ gas mass flow rate, lb/sec

$\dot{w}_w$ cooling water flow rate, lb/sec

Z axial distance measured from front surface of nozzle, ft

z axial distance along the column (ref. 4), ft

z_o $\dot{w}c_p/\pi k$ (ref. 4), ft

η efficiency

φ conductivity function, $\int k\,dT$, Btu/sec ft (reference value is -0.3 at 0^o R)

σ electrical conductivity, mho/ft

Subscripts

∞ value at large $\frac{z}{z_o}$

p pilot arc

M main arc

x heat exchanger

w typical water-cooled component

c downstream end of constrictor (Z = 0.23 ft)

APPARATUS AND DESIGN CONSIDERATIONS

Figure 3 is a sketch of the constricted-arc supersonic jet investigated. The plasma jet consists of three major parts: the upstream electrode, the constrictor nozzle, and the downstream electrode. Each of the components will be described and performance requirements will be discussed, starting with the central portion, the constrictor nozzle.

The Constrictor Nozzle

As the name suggests, the constrictor nozzle performs two functions. The cylindrical constrictor section produces the desired enthalpy and the smoothly contoured nozzle produces the desired supersonic flow. The diameter of the cylindrical constrictor is chosen to choke the desired mass flow at a desired pressure, and the length of it is sufficient to allow the stagnation enthalpy to approach a desired asymptotic value.

As explained in reference 4, the asymptotic enthalpy at a fixed gas flow rate increases with the ratio of arc current to constrictor diameter. The maximum enthalpy that can be achieved without burnout is limited ultimately by the maximum heat flux that can be absorbed by the constrictor wall. Thus, the wall of the constrictor nozzle must be adequately cooled along its length.

With gas and current specified, the arc-column voltage gradient imposed along the length of the tube increases both with mass flow and with the reciprocal of column diameter. To prevent short circuits, the constrictor nozzle is electrically insulated along its length to accommodate the impressed voltage gradient. Since sufficiently good heat conductivity and electrical insulation characteristics are mutually incompatible in a single material, the constrictor nozzle is a sandwich construction of alternate layers of insulating and heat-conducting material. The detail design of the constrictor nozzle is shown in figure 4. It consists of 13 water-cooled copper disks insulated from each other by 0.025-inch-thick wafers of hot-pressed boron nitride. The number of gaps (12) was selected to permit a nominal potential difference between adjacent copper disks of no more than 40 volts at open circuit conditions of the available power supply. The disks are 0.20 inch thick, except for the upstream- and downstream-end disks which are about 0.37 and 0.75 inch thick, respectively. Each disk is individually cooled with high-velocity water flow in an annular passage surrounding the central hole. The boron-nitride wafers are cooled by conduction to the copper disks. The disks are cemented together with an epoxy adhesive to provide a nonconducting, pressure-tight seal.

The Electrodes

The electrodes, although incidental to the behavior of the constrictor nozzle, are nevertheless important in the over-all performance and convenience of operation of the constricted-arc supersonic jet. Ideally, the electrodes: (1) should have sufficient current-carrying capacity; (2) should not contaminate the gas stream; (3) should not rely on or induce gas swirl or excessive turbulence; (4) should not disturb axial symmetry.

The upstream electrode.- A pointed, thoriated-tungsten cathode rod is used as the upstream electrode. The principal reason for the selection of tungsten is that the cathode spot attaches quietly to the incandescent tip and remains fixed in space on the axis of symmetry. Because a tungsten cathode requires an inert atmosphere, a shield of nitrogen is required if air or other chemically

active gas is to be heated. The flow rate of the protective gas can be much smaller than the main gas flow. For convenience, a commercially available plasma jet was used to provide the shield for the device of figure 3. Besides comprising the necessary shield, the commercial unit provides a pilot arc and enables convenient starting of the main arc.

The downstream electrode.- The downstream electrode operates in the low pressure environment associated with a supersonic flow. Consequently, the arc attachment process becomes diffuse, and the arc foot spreads over a relatively large area of the anode. A multiple-element, water-cooled copper anode serves to promote axial symmetry and to limit the local current density so that it is unnecessary to move the anode spots. Individual anode spots, each carrying about 75 amperes, can be maintained at a static pressure of 500 microns of mercury without erosion of the copper.

The anode consists of 6 water-cooled loops of 1/4-inch diameter copper tubing. The anode segments each require a ballast resistor to promote equal division of the current among the six electrode elements. The ballast resistors are connected to a common positive terminal as shown in figure 3. Even though individual ballast resistance of one ohm per segment is required, the total ballast resistance is only 1/6 ohm, owing to the parallel connection.

Instrumentation and Data Analysis

Measurements of the following quantities were carried out for the unit as a whole: total arc currents and voltages, cooling-water flow rates and temperature rises, gas flow rates, and static pressures upstream of the constrictor nozzle. Detailed measurements were also made of the voltage drops between the cathode and the various constrictor-nozzle disks and of the cooling-water flow rates and water-temperature rises for each of the disks. Figure 5 is a schematic drawing of the arrangement of the instrumentation.

The data-reduction technique is described in appendix A. Briefly, it consists of performing a balance between the electric power delivered to the electric arc and the power losses to the various water-cooled parts which surround the jet. The power balance can be determined locally for a portion of the constrictor nozzle, or it can be determined over-all for the entire system. The power absorbed by the downstream heat exchanger furnished data for comparison with the over-all power balance. Enthalpy is calculated by dividing the power absorbed in the gas by the measured gas flow.

RESULTS AND DISCUSSION

The constricted-arc supersonic jet was operated over a range of currents from 108 to 240 amperes and nitrogen flow rates from 3.1×10^{-4} to 11.4×10^{-4} lb/sec in order to determine the performance. The corresponding power input varied from 35 to 55 kw. It was convenient to use nitrogen for the majority of the tests, since the entire flow could be put through the pilot arc. Because recent

calculations (refs. 5 to 9) show that air and nitrogen have similar high-temperature properties (see figs. 6 and 7), it is believed that the results of tests with nitrogen should agree qualitatively with results for air. For the purpose of testing this hypothesis, a mixture of 38-percent N_2 and 62-percent air by weight was used in some tests. The data points for this mixture are flagged on the performance curves that follow.

Over-all Measurements

The over-all measurements represent average values at the downstream end of the constrictor section of the nozzle (Z = 0.23 ft). Measurements made downstream of the cylindrical constrictor tube exhibited considerable scatter and gave evidence of the possible existence of nonrepeatable modes of arc operation within the supersonic region. Since most of the total enthalpy rise occurs in the constrictor tube, the performance as evaluated at the downstream end of the constrictor is considered to be of most interest.

Constrictor voltage.- The constrictor voltage, defined as the voltage with respect to the cathode of the disk at Z = 0.23 feet, is a function of arc current and nitrogen flow rate. As is shown in figure 8, the voltage variation with current is small, being approximately 10 volts over a current range from 90 to 240 amperes. For a given flow, the curve exhibits a slight negative slope at currents below about 140 amperes and a slight positive slope at currents above 140 amperes. As is shown in figure 9, the increase in voltage with flow rate is about 25 volts for a twofold mass flow rate increase, and is approximately linear for the flow range covered.

Total enthalpy.- The average total enthalpy of the gas which passed the constrictor was determined by the power balance technique described in appendix A. Figure 10 shows enthalpy so determined as a function of nitrogen flow rate for various currents. The plotted points indicated that enthalpies in excess of 28,000 Btu/lb were achieved with currents of the order of 240 amperes and mass flows of 7×10^{-4} lb/sec. The over-all enthalpy varies approximately as the first power of current and decreases with increasing flow rate. This behavior is further illustrated in figure 11 where the ratio of enthalpy to current is plotted as a function of flow rate.

The heat balance enthalpy was compared, for some of the runs, with the enthalpy obtained by measuring the power absorbed by the heat exchanger (fig. 5). Results of typical comparisons are listed below:

I, amp	$\dot{w}$ lb/sec$\times10^4$	H (power - losses), Btu/lb	H (heat exchange), Btu/lb
138	7.4	14,500	13,900
135	4.4	15,000	14,100
185	7.4	21,100	17,000

The agreement between the two methods is quite satisfactory, especially at the two lower currents, where the runs were long enough for the heat exchanger to

reach equilibrium. The heat balance losses do not include those through the uncooled windows (fig. 3). (The windows, in fact, limited the permissible current and the duration of the runs.) Therefore, the enthalpy computed by the heat-balance method tends to be high. Moreover, the short section of duct just upstream of the heat exchanger (fig. 5) was not instrumented to measure heat loss. Thus, the enthalpy deduced from the heat captured by the exchanger tends to be low. The true average enthalpy would be expected to lie somewhere between the two listed values.

Efficiency.- The efficiency of the constrictor is defined as the ratio to the electric power delivered to the arc of the power remaining in the gas at the downstream end of the constrictor tube ($Z = 0.23$). The efficiency, the electric power delivered to the gas, and the power remaining in the gas for a current of 183 amperes are shown in figure 12(a). All three quantities, the power delivered, the power remaining, and their ratio, the efficiency, increase with increasing nitrogen flow rate. The constrictor efficiency for a range of currents is given in figure 12(b). It can be seen that efficiency is insensitive to current but is a strong function of gas flow rate.

Stagnation chamber pressure.- The highest enthalpies were achieved at subatmospheric stagnation pressures. Static pressure measured in the stagnation chamber upstream of the constrictor nozzle is shown in figure 13 as a function of flow rate and current. The pressure ranged from about 1/4 to 3/4 atmosphere for currents from 108 to 240 amperes and flow rates from 3.1×10^{-4} to 11.5×10^{-4} lb/sec. Since the constrictor nozzle operates aerodynamically choked, the pressure cannot be controlled independently, but increases with increasing flow rate and current. The pressure and gas flow rate per unit constrictor area can be correlated with enthalpy as shown in figure 14. The parameter $\dot{w}/A^*p_o$ is approximately proportional to $H^{-0.4}$, which one would deduce for one-dimensional, equilibrium isentropic, critical flow (see ref. 10).

Local Measurements

Detailed measurements of voltage and wall heat flux along the constrictor were reduced using techniques described in appendix A. It is instructive to examine the distribution with length of these quantities to understand the local rates of heat generation and heat loss. These measurements also provide a basis for a comparison of experimental data with theory.

Local voltage.- Since the current is constant along the length of the constrictor, the voltage developed between the cathode and any disk is a measure of the electric power delivered to the flowing gas up to the disk location. As in the discussion of figures 8 and 9, where the over-all arc voltage was shown to be relatively independent of current but strongly dependent on gas flow rate, the voltage is insensitive to current change at a fixed flow rate. However, it increases strongly with increasing flow rate at fixed current (fig. 15).

Wall heat flux.- According to reference 4, the distribution of wall heat flux with length will vary directly with the enthalpy in the cylindrical portion

of the constrictor nozzle. Therefore, the maximum cooling rate that can be established at the wall determines the maximum enthalpy that can be contained. Typical heat flux distributions with length are illustrated in figure 16 for various currents and gas flow rates. The heat flux is moderate near the upstream end of the constrictor nozzle and rises at a decreasing rate toward a maximum value near the downstream end of the cylindrical portion. The heat flux then decreases in the supersonic region. The thermal conduction between disks was neglected; however, it may be appreciable where large axial temperature gradients exist in the disks, such as at the entrance of the divergent section of the nozzle. Therefore, the actual wall heat flux may not decrease near the entrance to the divergent section as does the measured wall heat flux illustrated in figure 16. The highest heat flux, about 1650 Btu/sec ft^2, is associated with high current and low mass flow, whereas the lowest maximum heat flux shown, 1100 Btu/sec ft^2, was obtained with low current and high mass flow.

Local total enthalpy.- The distribution of enthalpy along the length of the constrictor nozzle can be deduced from the voltage and wall heat flux measurements. The enthalpy, defined as the net power stored in the gas divided by the gas flow rate, represents an average of whatever radial distribution exists. By means of the one-dimensional power balance, it is found that the change of power absorbed by the gas per unit length is equal to the difference between the electric power delivered per unit length and the loss per unit length:

$$d(\dot{w}H)/dZ = \dot{w}\, dH/dZ = EI/1054 - \pi Dq$$

Measured values of the two terms in the right-hand side are plotted as a function of length in figure 17 for a typical run. The difference between the two experimental curves, the power gradient, is proportional to the enthalpy gradient, since the mass flow does not depend on length. A relatively high enthalpy gradient occurs at the constrictor inlet. The enthalpy gradient drops to a minimum value near the downstream end of the constrictor, and increases in the expanding portion of the nozzle.

The integrals with respect to length of the curves of figure 17 are shown in figure 18. As is indicated on the figure, the difference between the two experimentally determined curves is proportional to the net power delivered to the gas, from which the enthalpy can be computed by dividing by the measured mass flow. The computation neglects the enthalpy of the cold gas which enters the system.

The variation of enthalpy with length along the constrictor is shown in figure 19 for several values of current and flow rate. The enthalpy level and the rate at which it increases is a function of the current and flow rate. The enthalpy rises more quickly at low flow rates and in some cases reaches an asymptotic value in the constrictor tube. A further increase in enthalpy takes place as the gas leaves the constant area (throat) section and enters the divergent (supersonic) region of the nozzle. The change occurs near $Z = 0.23$ foot and is the result of the apparent drop in the power loss to the wall (fig. 16).

No doubt exists that the exit flow is supersonic, since luminous shock diamonds are clearly visible in the discharge, and bow-shock waves are formed

ahead of blunt obstacles placed in the jet. The addition of heat to the expanding, supersonic flow apparently allows the total enthalpy to increase while the static enthalpy remains at a relatively low value. Although heat addition in the supersonic flow would tend to alleviate the radiation loss that would otherwise eventually limit enthalpy obtainable in the constrictor, Cann (ref. 11) concludes that heating in the supersonic flow would result in only marginal gains in the stagnation enthalpy. At the very least, the electric discharge through the diverging section appears to prevent the cooling of the plasma which would otherwise occur.

Comparison of Experiment With Theory

In reference 4, Stine and Watson propose that the characteristics of the constricted arc may be approximated by an analytical model that neglects all heat losses except radial thermal conduction. Furthermore, the functional relationships between the three state properties of the gas, enthalpy, thermal conductivity potential, and electrical conductivity are linearized as is illustrated in figures 6 and 7. The theory predicts that the variables current, pressure, gas flow rate, constrictor length, constrictor radius, and gas properties do not all affect the characteristics of the constricted arc independently; rather, the characteristics are dependent only on various groupings of the parameters. Enthalpy at any position in the arc column can be expressed as a function of I/r_e, $c_p/kA^{1/2}$, $z/(\dot{w}c_p/\pi k)$, and r/r_e; the heat flux at any position on the constrictor wall can be expressed as a function of $I/r_e{}^2A^{1/2}$ and $z/(\dot{w}c_p/\pi k)$ (or alternatively as a function of Hk/c_p only), and the voltage gradient can be expressed as a function of $r_eA^{1/2}$ and $z/(\dot{w}c_p/\pi k)$.

The experimental data will now be compared with the theory to determine whether or not the theoretical model approximates the constricted arc and to determine whether or not the various groupings of parameters reduce the experimental data. Comparisons involving the parameter r/r_e cannot be carried out because measurements of the radial enthalpy distributions in the constrictor were not made; only the radially averaged enthalpy was determined. Furthermore, various theoretical calculations of gas properties disagree, especially with regard to the thermal conductivity potential (e.g., refs. 6 and 8). Thus, unambiguous values of the terms c_p/k and A, the slopes of the straight-line approximations shown in figures 6 and 7, respectively, cannot be selected. The factors c_p/k and A are therefore deleted from the parameters. The incomplete parameters will, however, permit a comparison of the experiment with theory for a particular working gas, in this case nitrogen. After the particular comparison is made, the experimental determination of values of c_p/k and A which will enable a quantitative comparison with theory will be discussed. In what follows, the origins of the experimental (Z) and theoretical (z) axes are assumed to coincide, despite evidence that the effective origin of the constrictor migrates downstream as mass flow increases.

Figure 20 shows the product of voltage gradient and constrictor radius as a function of $z/\dot{w}$. A curve with a shape prescribed by theory and with an

asymptotic value selected to best fit the data also is shown. It should be noted that the theory predicts that the voltage gradient will be independent of current and will be a strong function of flow rate and axial position. The comparison shown on figure 20 suggests that current does not strongly affect the voltage gradient but, rather, that the parameter $z/\dot{w}$ is indeed the important variable.

Figure 21 shows the constrictor wall heat flux as a function of average enthalpy. The enthalpy was selected as the parameter rather than I/r_e^2 and $z/\dot{w}$ in order to more easily discuss the assumption that radial heat conduction is the dominant form of heat loss. The gas flow rates are listed beside each data point. The straight line prescribed by theory is assigned a slope which best fits the data. The theory predicts that the heat loss will be a linear function of enthalpy and will be independent of flow rate. The data show the linear variation of constrictor wall heat flux with enthalpy predicted by the theory. The data further illustrate that radial heat conduction is the dominant form of heat loss at the moderate pressures of the tests. If radiation were important as a loss mechanism, the heat flux would increase more strongly than linearly with enthalpy, and if turbulent convection were important, the heat flux would increase with increasing flow rate.

The selection of the asymptotic value of the curve in figure 20 and the selection of the slope of the straight line in figure 21 determines the values of A and c_p/k, respectively, which allow a quantitative agreement of experiment with theory. These values can now be compared with the theoretically calculated values in figures 7 and 6. The straight-line approximations shown in these figures were, in fact, drawn after the experimentation and possess the slopes A and c_p/k, respectively, which were obtained from figures 20 and 21. These values give reasonable straight-line approximations to the theoretical calculations of gas properties by Hansen (ref. 5), Viegas and Peng (ref. 7), Ahtye (ref. 6), and Yos (ref. 8).

The experimentally determined enthalpy, shown as a function of the parameters I/r_e, $c_p/kA^{1/2}$, and $z/(\dot{w}c_p/\pi k)$, is compared in figure 22 with the enthalpy predicted by the theory. (For average enthalpies in excess of 10,000 Btu/lb, $r_w \approx r_e$; so I/r_w can be substituted for I/r_e.) The comparison illustrates that the theory correctly predicts the increase of enthalpy with axial distance and correctly predicts the dependence of enthalpy on current. It should be noted that one can use this theoretical curve to aid in the selection of a constrictor length which gives high enthalpy without unreasonable heat loss. For values of $z/(\dot{w}c_p/\pi k)$ greater than 0.3, the heat losses are large and the increase in enthalpy with axial distance is small. For $z/(\dot{w}c_p/\pi k)$ less than 0.05 the enthalpy of the gas is much less than the asymptotic value. A constrictor length equal to 0.2 $(\dot{w}c_p/\pi k)$ gives a high enthalpy with moderate heat loss.

The theory, therefore, agrees with the experiment for the 1/4-inch diameter constricted arc with nitrogen and air, and the parameters suggested do reduce the experimental data. The theory will have to be compared with experiments in

constrictors of different diameters in order to test the scaling laws predicted by the theory over the range of sizes for which the analytical model is a reasonable approximation.

Ames Research Center
National Aeronautics and Space Administration
Moffett Field, Calif., Oct. 4, 1963

APPENDIX A

INSTRUMENTATION AND CALCULATIONS

To provide data for comparison with the theory of reference 4, the performance of the constricted-arc supersonic jet was evaluated at various locations within the cylindrical constrictor. Both the electric power supplied to the arc and the power losses to the various water-cooled parts were measured, and the power absorbed by the gas was obtained by subtraction. The total enthalpy was then determined as the net power divided by the gas flow rate. Measurements were made of the voltage between the cathode and the downstream end of the constrictor and of the total heat loss up to that point to provide data for an over-all enthalpy determination. In addition, the voltages appearing on, and heat losses of the various insulated sections of the constrictor were measured to provide information for determining local values of total enthalpy. Figure 5 is a schematic drawing of the instrumentation employed for the heat-balance measurements.

OVER-ALL MEASUREMENTS AND CALCULATIONS

Steady-state measurements were made of the following quantities: voltage, current, gas flow rate, static pressure in the upstream plenum chamber, and power loss to the various water-cooled parts. Voltages and currents were measured with meters having D'Arsonval type movements. A precision resistor in the voltmeter circuit and a precision shunt in the ammeter circuit limited measuring errors to 1/2 percent of full scale. The gas flow rate was measured by a calibrated rotometer and the pressure upstream of the constrictor nozzle was measured with a differential pressure gage. A mechanical vacuum pump provided a reference pressure of 6 microns of mercury that was negligible with respect to pressures being measured.

The power absorbed by the water-cooled parts was calculated from the cooling water flow rates and the temperature rises. The flow rates were read on calibrated rotometers; the temperature rises were measured by means of differential temperature transducers of the type described in reference 12. The temperature signals were displayed on a 10-millivolt self-balancing potentiometer recorder.

The total power delivered to the system was calculated in the following way. The arc power was obtained by adding the product of the pilot-arc current and voltage to the product of the constrictor-arc voltage and main arc current. The constrictor voltage was measured between the cathode and the constrictor disk at $Z = 0.23$ foot.

The net power absorbed by the gas was taken as the difference between the total electric power delivered and the power absorbed in the cooling water. The over-all total enthalpy was obtained by dividing the net power by the gas flow rate.

For comparison, another over-all constrictor enthalpy, based on the power absorbed by the heat exchanger, was calculated for some of the runs. The power absorbed by the supersonic portion of the nozzle was added to that of the heat exchanger, whereas the power delivered to the gas, the product of main current and the difference between the anode voltage and that at the downstream end of the constrictor, was subtracted from the above sum to give the net power at the constrictor exit. The heat-exchanger enthalpy is then expressed as follows:

$$H_x = \frac{\dot{w}_w \Delta T_x}{\dot{w}} + \frac{P_{nozzle}}{\dot{w}} + \frac{P_{anode}}{\dot{w}} - \frac{V_{anode} - V_c}{1054\ \dot{w}} I$$

LOCAL MEASUREMENTS AND CALCULATIONS

As shown in figure 5, the constrictor nozzle was instrumented to allow a local heat balance and thus to allow determination of the longitudinal distributions of enthalpy. The net power remaining in the gas at any longitudinal position was given by the electrical power delivered to the gas, minus the total losses to the water-cooled constrictor disks and other cooled parts upstream of that point.

The electric power delivered to the gas was taken to be the product of the main arc current and the voltage difference which appeared between the cathode and a particular constrictor disk. One voltmeter was switched in turn to each of the 13 copper disks to obtain these measurements.

The power absorbed by each disk was determined by measuring the temperature rise of the cooling water with an iron-constantan differential thermocouple pair. The cooling water flow rate was determined in a prerun calibration by weighing the water that passed through the cooling passages of each disk during a given time.

REFERENCES

1. John, Richard R., and Bade, William L.: Recent Advances in Electric Arc Plasma Generation Technology. ARS Jour., vol. 31, no. 1, Jan. 1961, pp. 4-17.

2. Finkelnburg, W., and Maecker, H.: Elektrische Bögen und Thermisches Plasma. Handbuck der physik, vol. XXII, Julius Springer (Berlin), 1956, pp. 254-444.

3. Maecker, H.: Thermal and Electrical Conductivity of Nitrogen up to 15000° K by Arc Measurements. Paper presented at AGARD Conf. on Properties of Gases at High Temperature, Aachen, Germany, Sept. 21-23, 1959.

4. Stine, Howard A., and Watson, Velvin R.: The Theoretical Enthalpy Distribution of Air in Steady Flow Along the Axis of a Direct-Current Electric Arc. NASA TN D-1331, 1962.

5. Hansen, C. Frederick: Approximations for the Thermodynamic and Transport Properties of High-Temperature Air. NASA TR R-50, 1959.

6. Ahtye, Warren F., and Peng, Tzy-Cheng: Approximations for the Thermodynamic and Transport Properties of High-Temperature Nitrogen with Shock-Tube Applications. NASA TN D-1303, 1962.

7. Viegas, John R., and Peng, T. C.: Electrical Conductivity of Ionized Air in Thermodynamic Equilibrium. ARS Jour., vol. 31, no. 5, May 1961, pp. 654-657.

8. Yos, Jerrold M.: Transport Properties of Nitrogen, Hydrogen, Oxygen, and Air to 30,000° K. Res. and Adv. Dev. Div., Avco Corp., RAD-TM-63-7, Mar. 1963.

9. Maecker, H.: The Properties of Nitrogen up to 15,000° K. AGARD Report No. 324, Sept. 1959.

10. Shepard, Charles E., and Winovich, Warren: Electric-Arc Jets for Producing Gas Streams with Negligible Contamination. ASME Paper No. 61-WA-247, presented at New York City, Nov. 26-Dec. 1, 1961.

11. Cann, G. L., Teem, J. M., Buhler, R. D., and Branson, L. K.: Magnetogasdynamics Accelerator Techniques. AEDC-TRD-62-145, July 1962, p. 31.

12. Wald, David: Measuring Temperature in Strong Fields. Instruments and Control Systems, vol. 36, no. 5, May 1963, pp. 100-101.

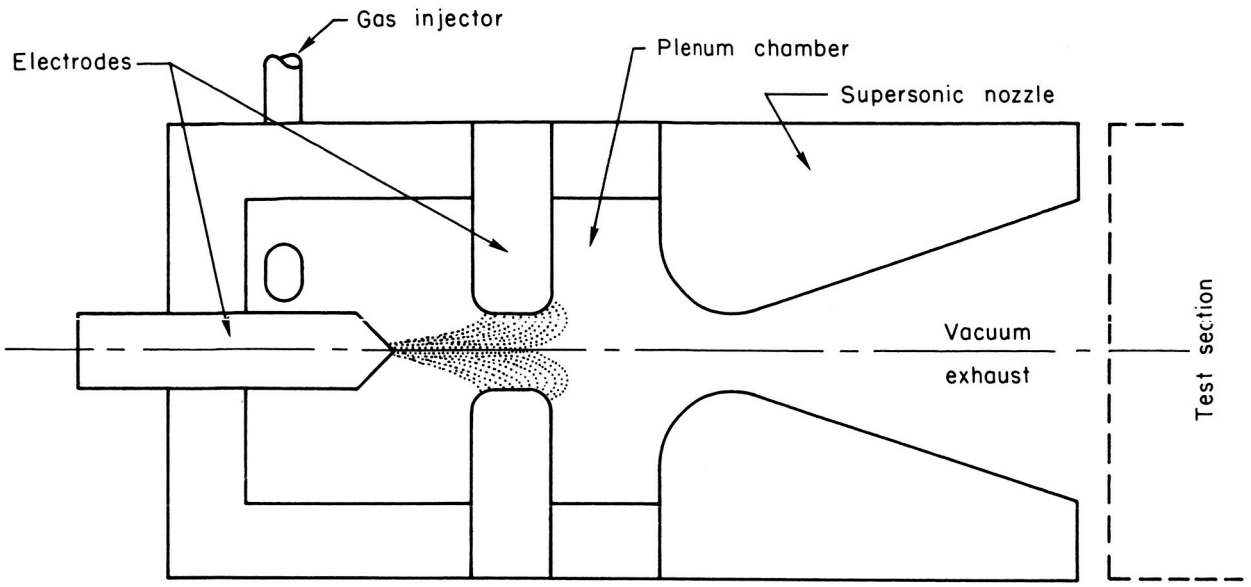

Figure 1.- Conventional arc-heated supersonic jet.

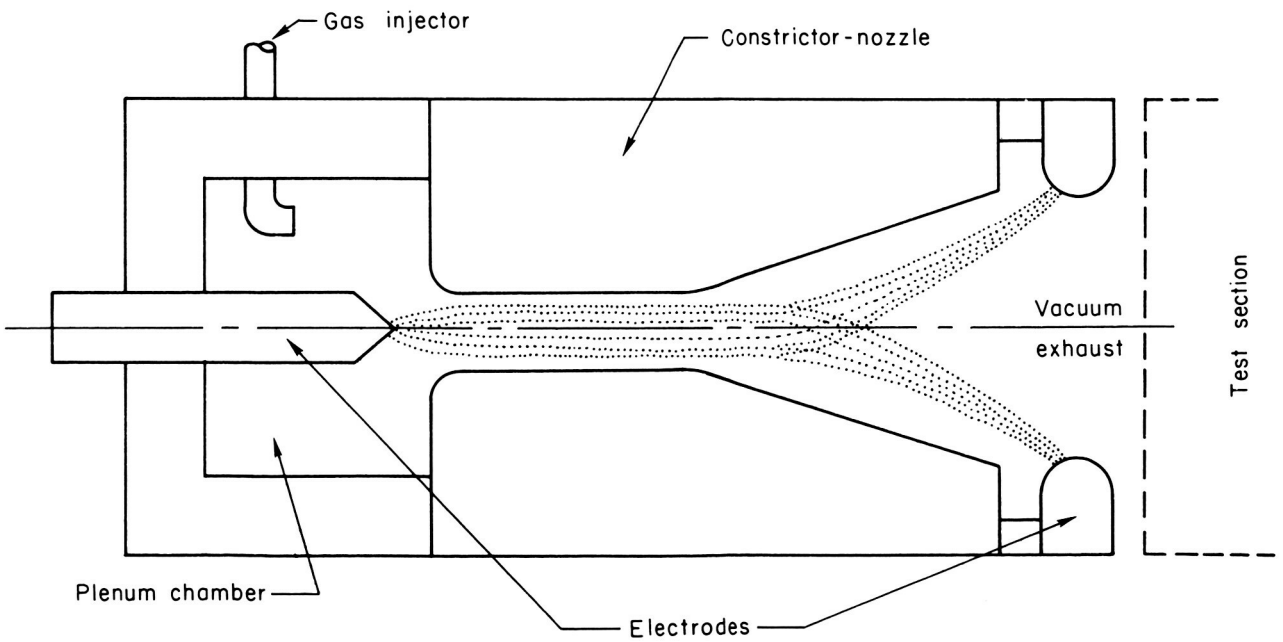

Figure 2.- The constricted-arc supersonic jet.

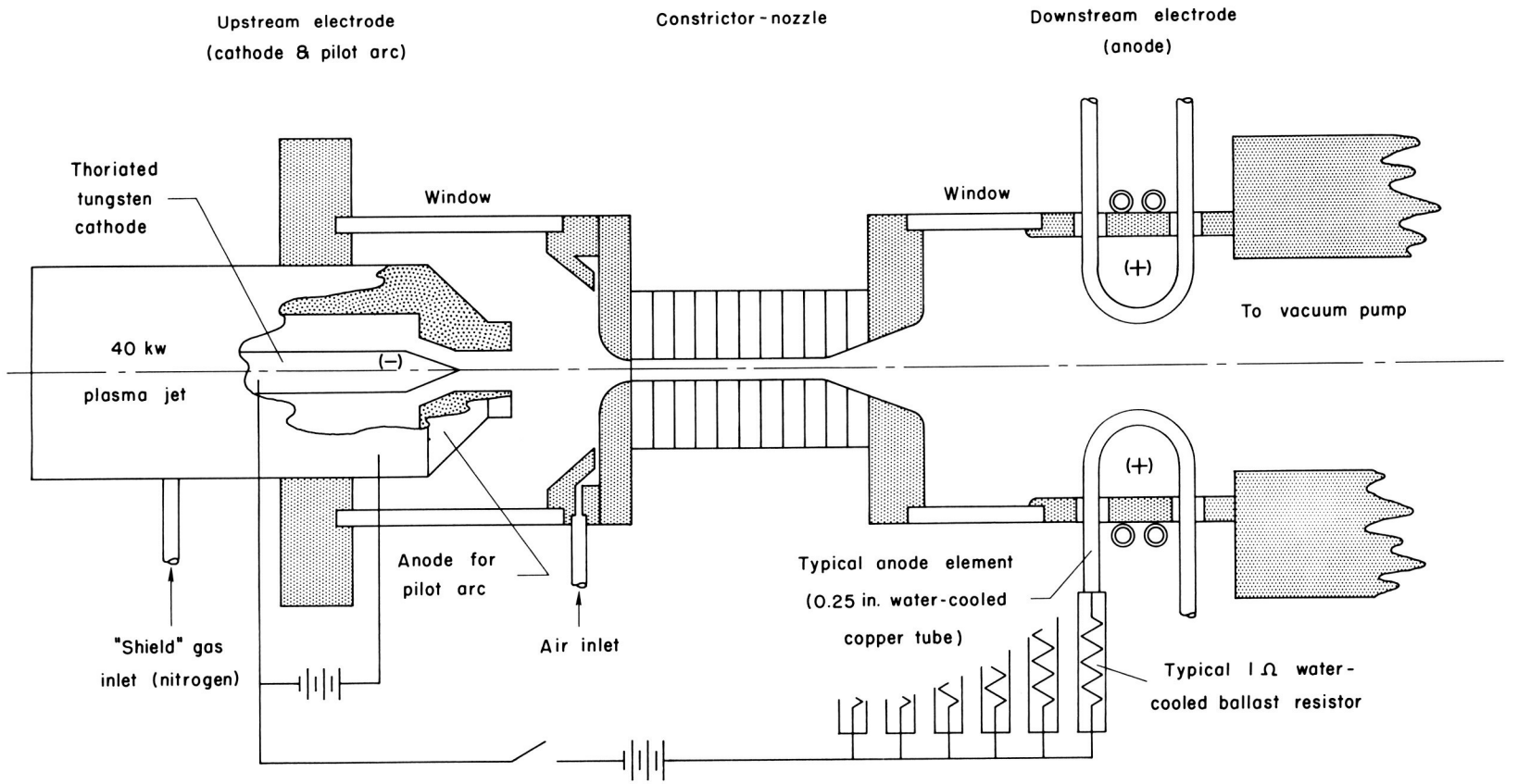

Figure 3.- Arrangement of components of constricted-arc supersonic jet.

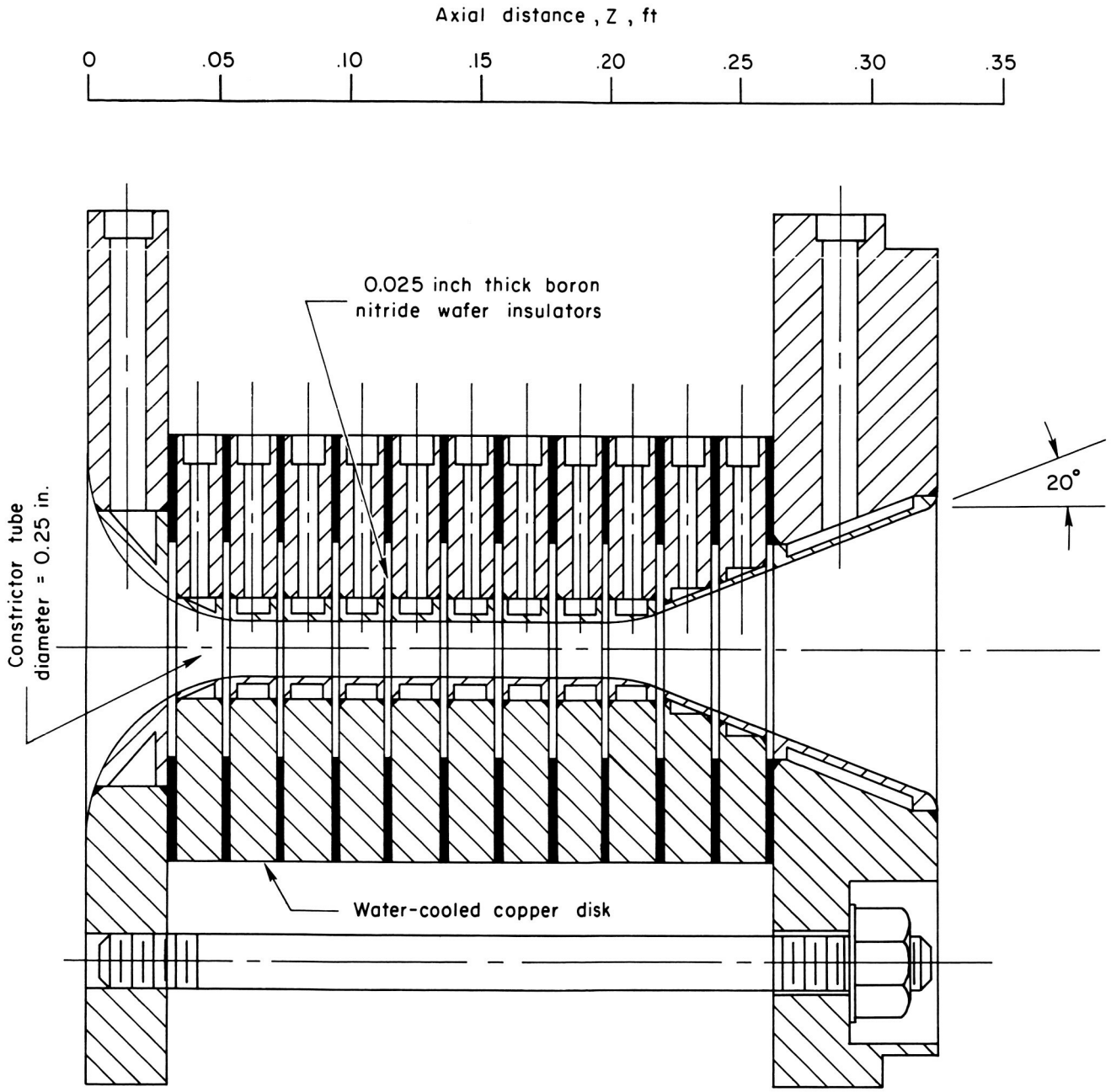

Figure 4.- Detail of constrictor nozzle.

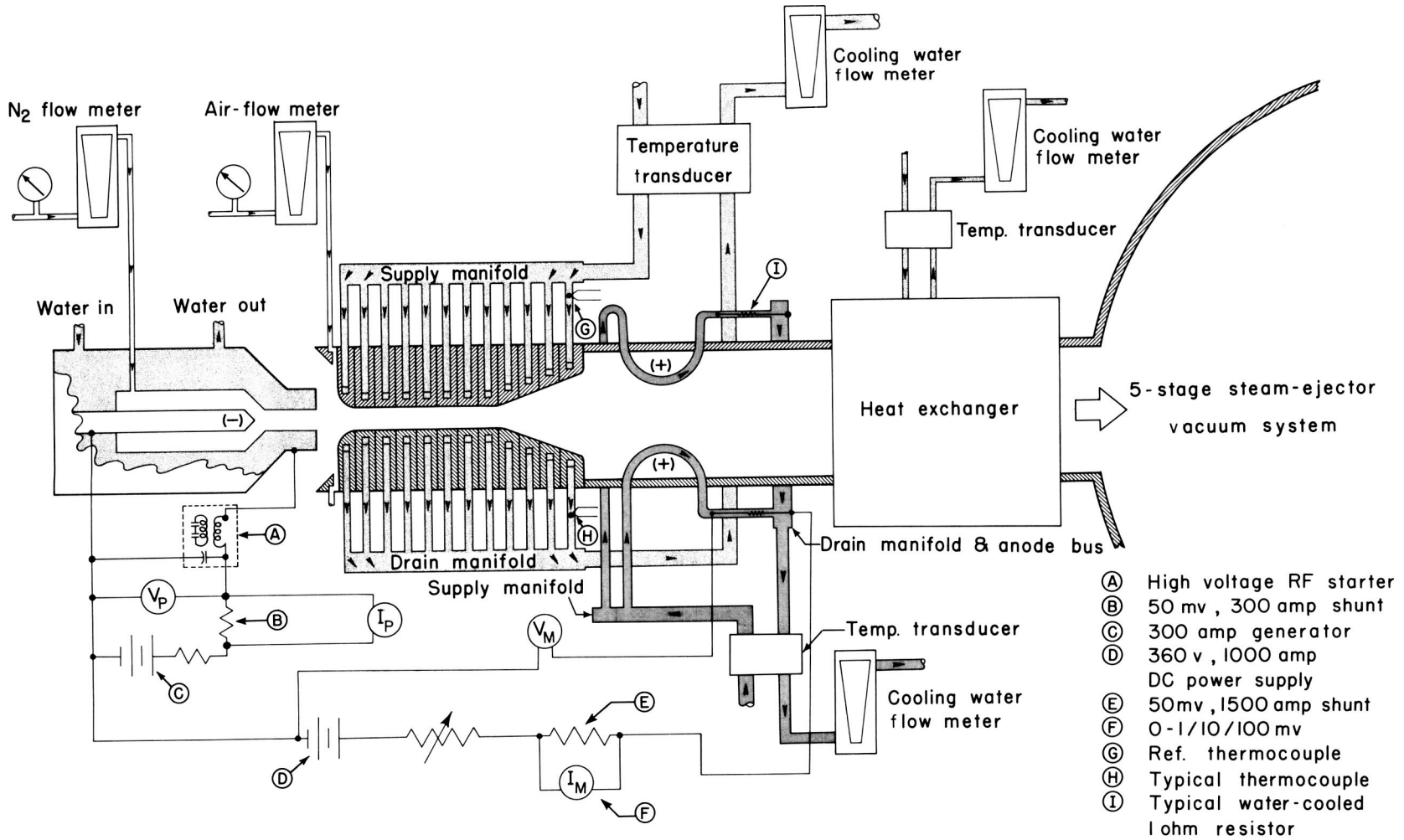

Figure 5.- Instrumentation for the constricted-arc supersonic jet.

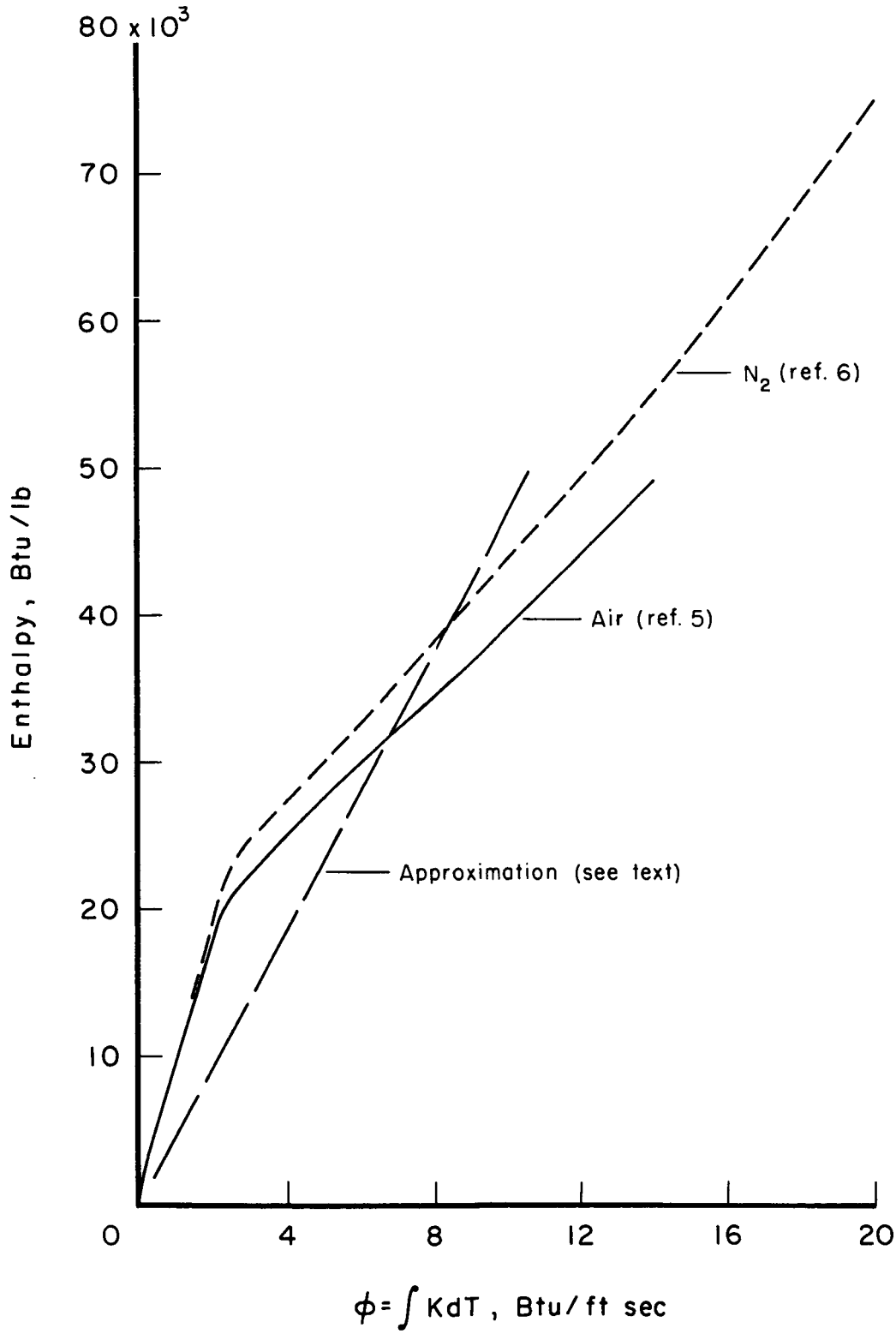

Figure 6.- Enthalpy as a function of thermal conductivity potential for air and nitrogen at 1 atmosphere.

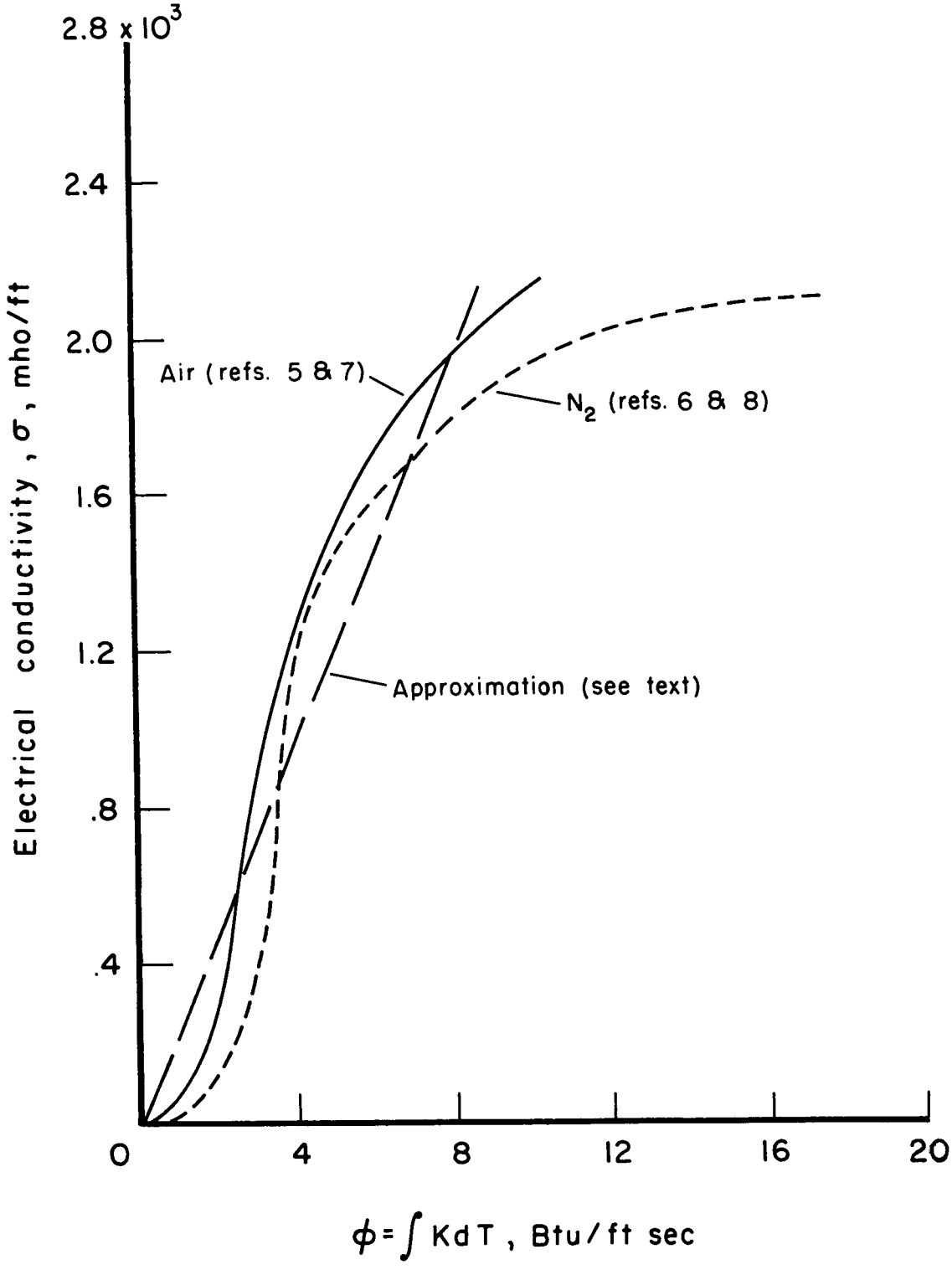

Figure 7.- Electrical conductivity as a function of thermal conductivity potential for air and nitrogen at 1 atmosphere.

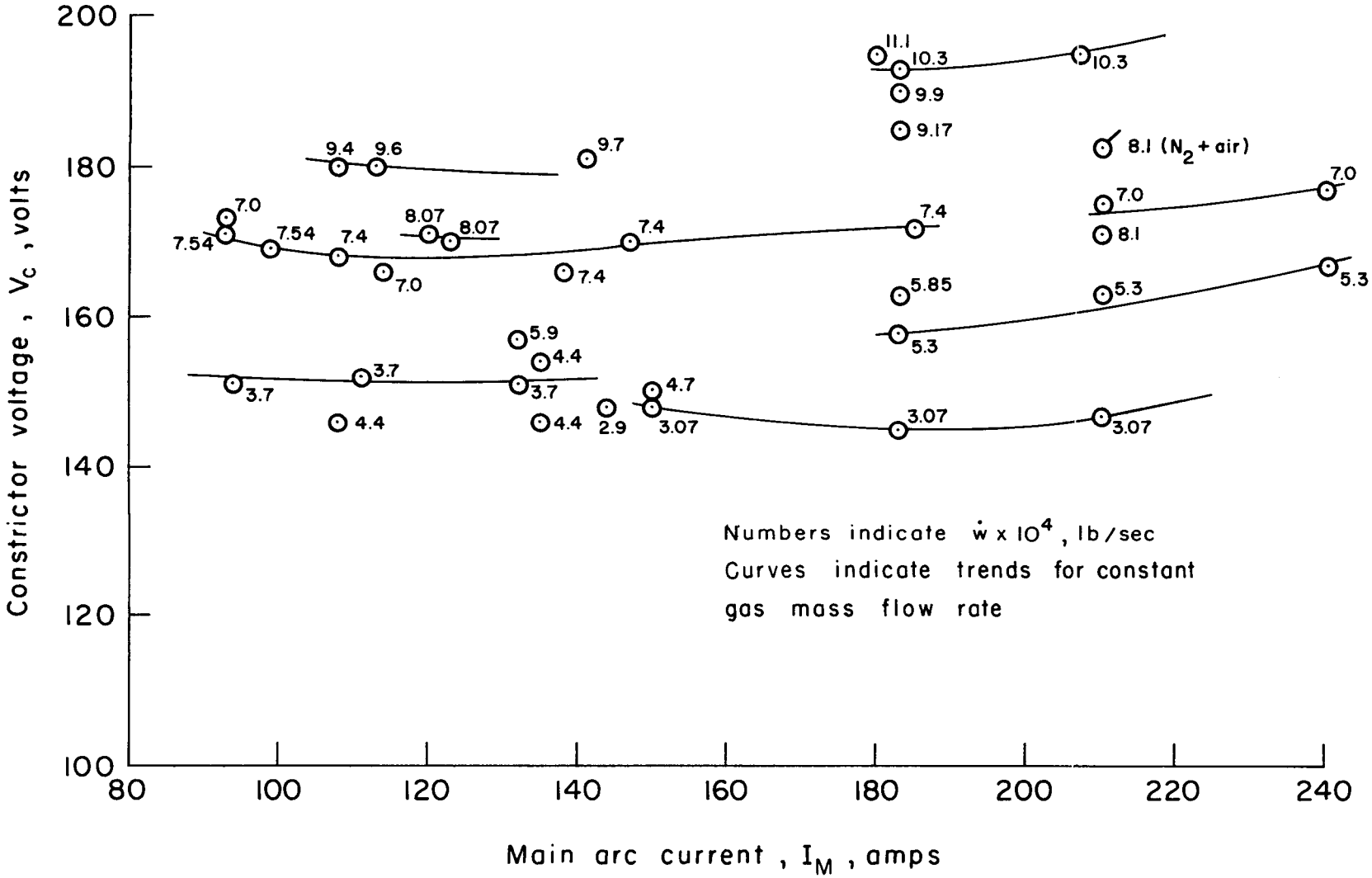

Figure 8.- Constrictor voltage versus arc current for various flow rates.

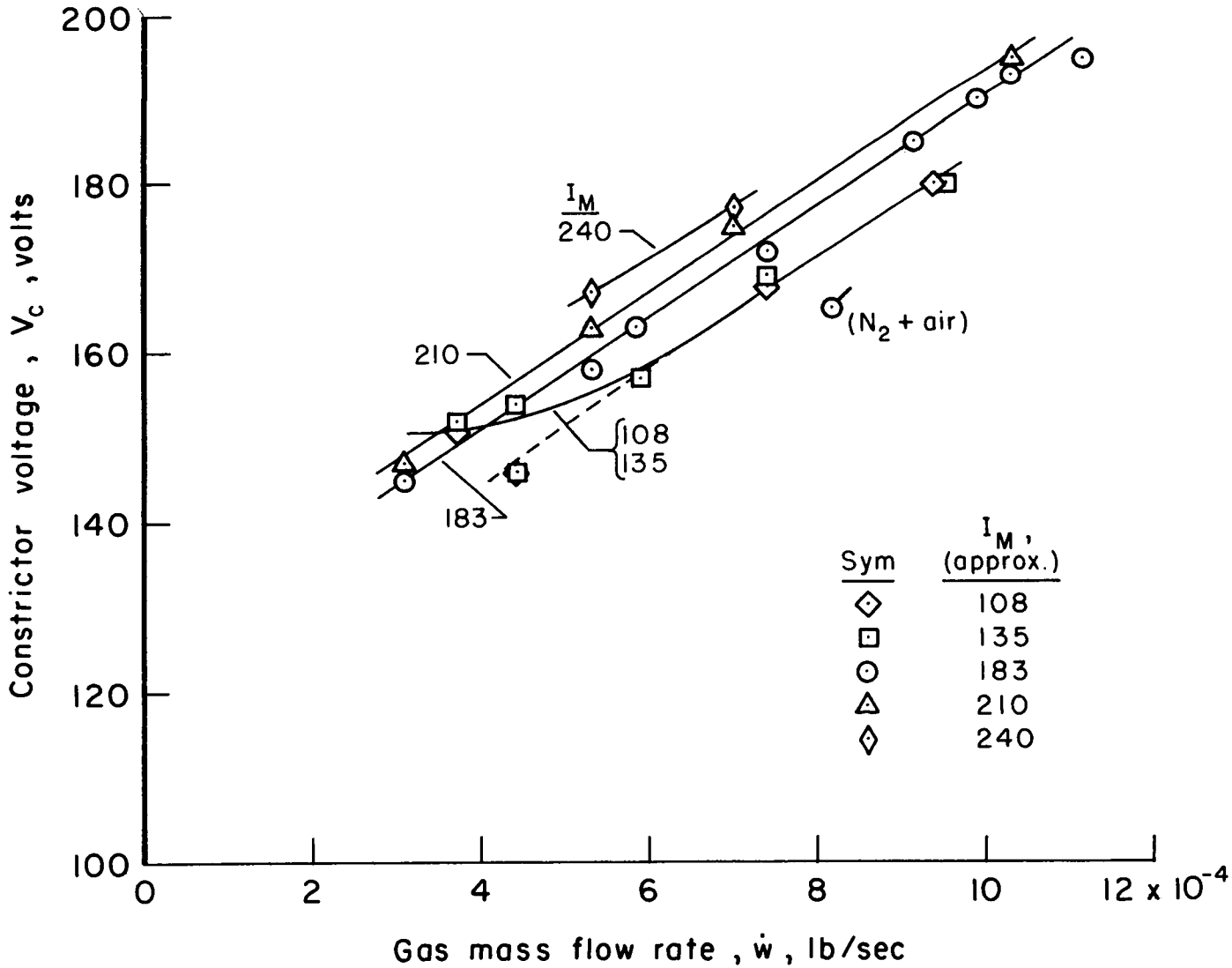

Figure 9.- Constrictor voltage versus nitrogen flow rate for various arc currents.

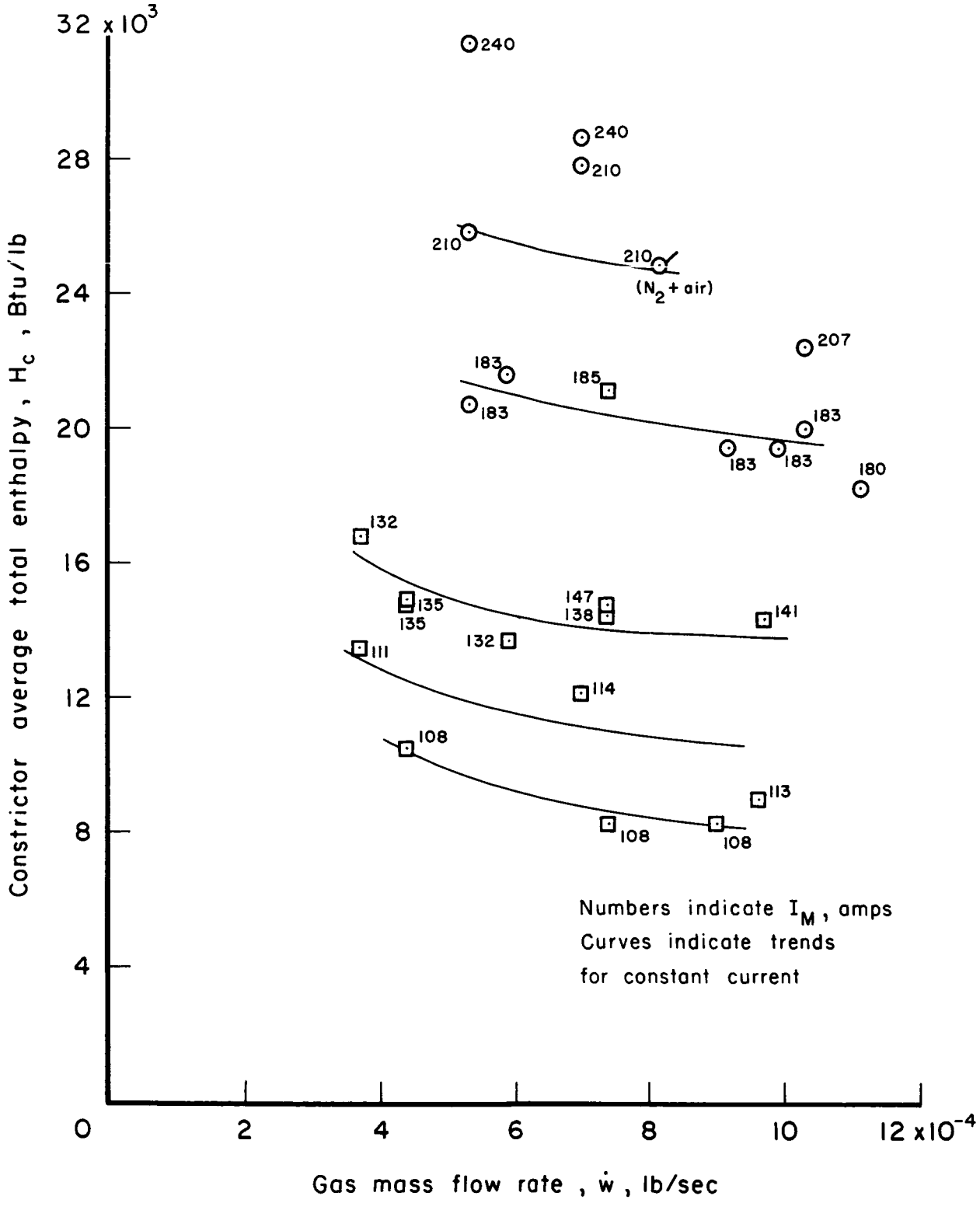

Figure 10.- Constrictor average total enthalpy versus nitrogen flow rate for various arc currents.

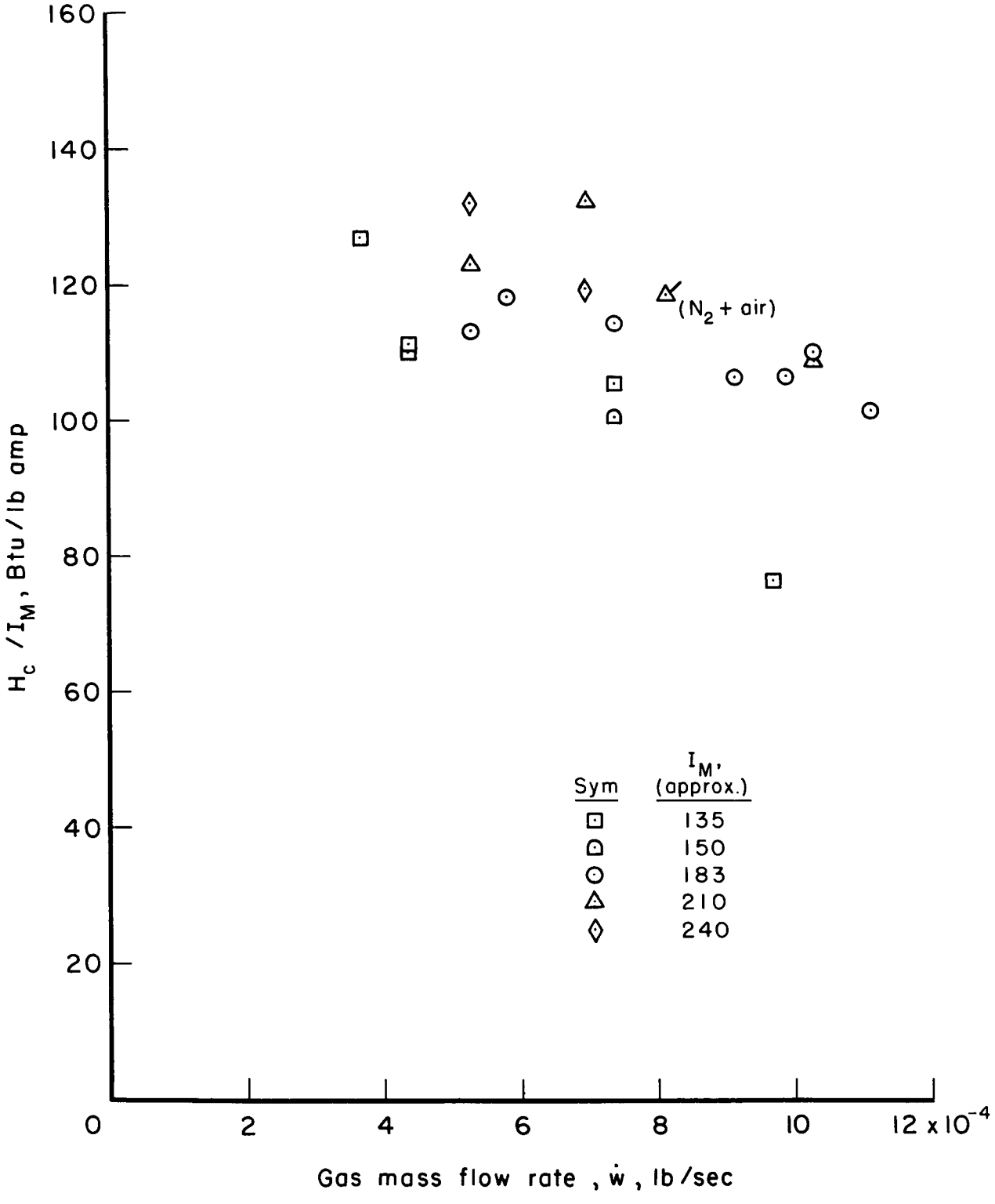

Figure 11.- Average constrictor enthalpy per unit arc current versus nitrogen flow rate.

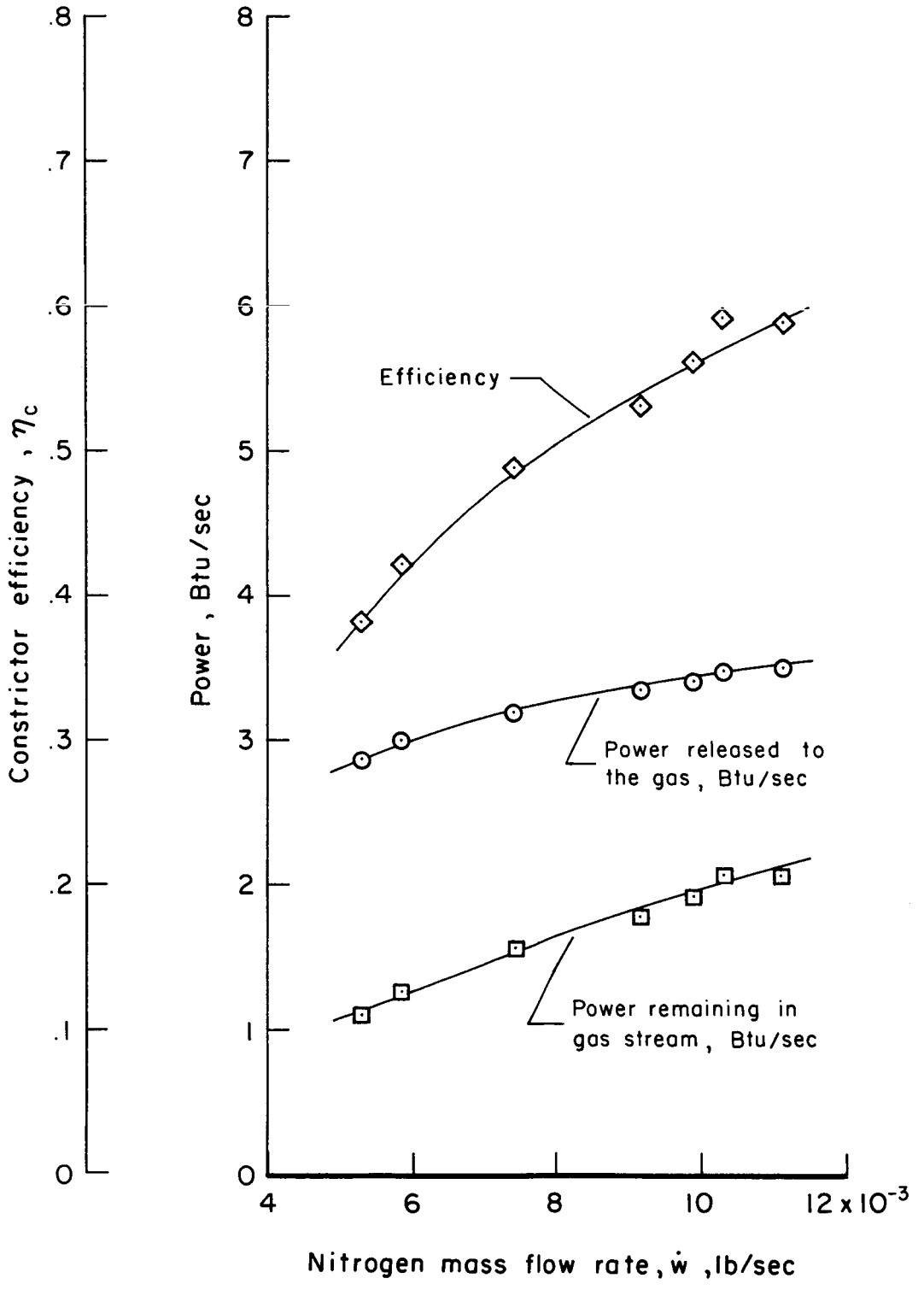

(a) I_M = 183 amp

Figure 12.- Power and constrictor efficiency versus nitrogen flow rate.

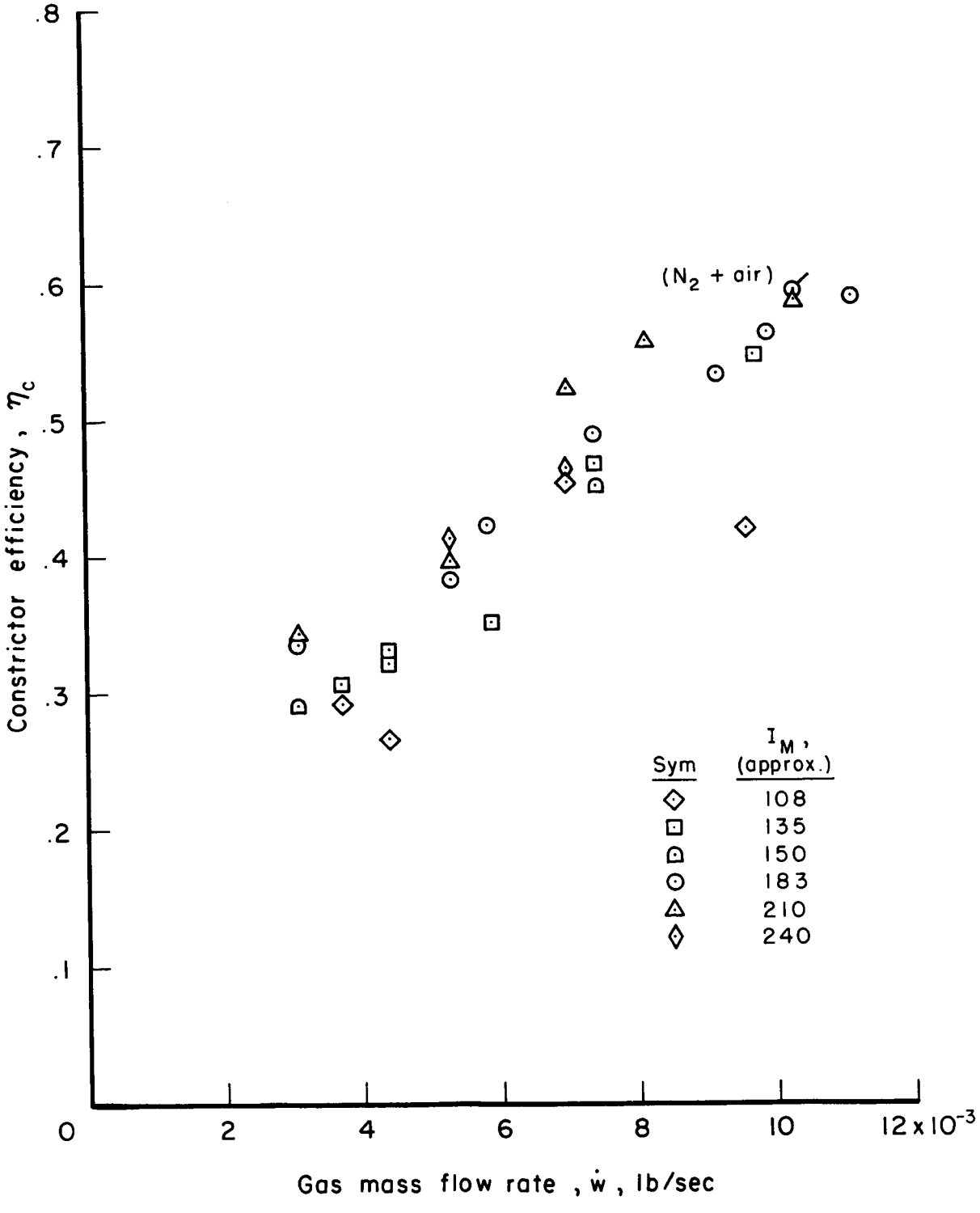

(b) Various arc currents.

Figure 12.- Concluded.

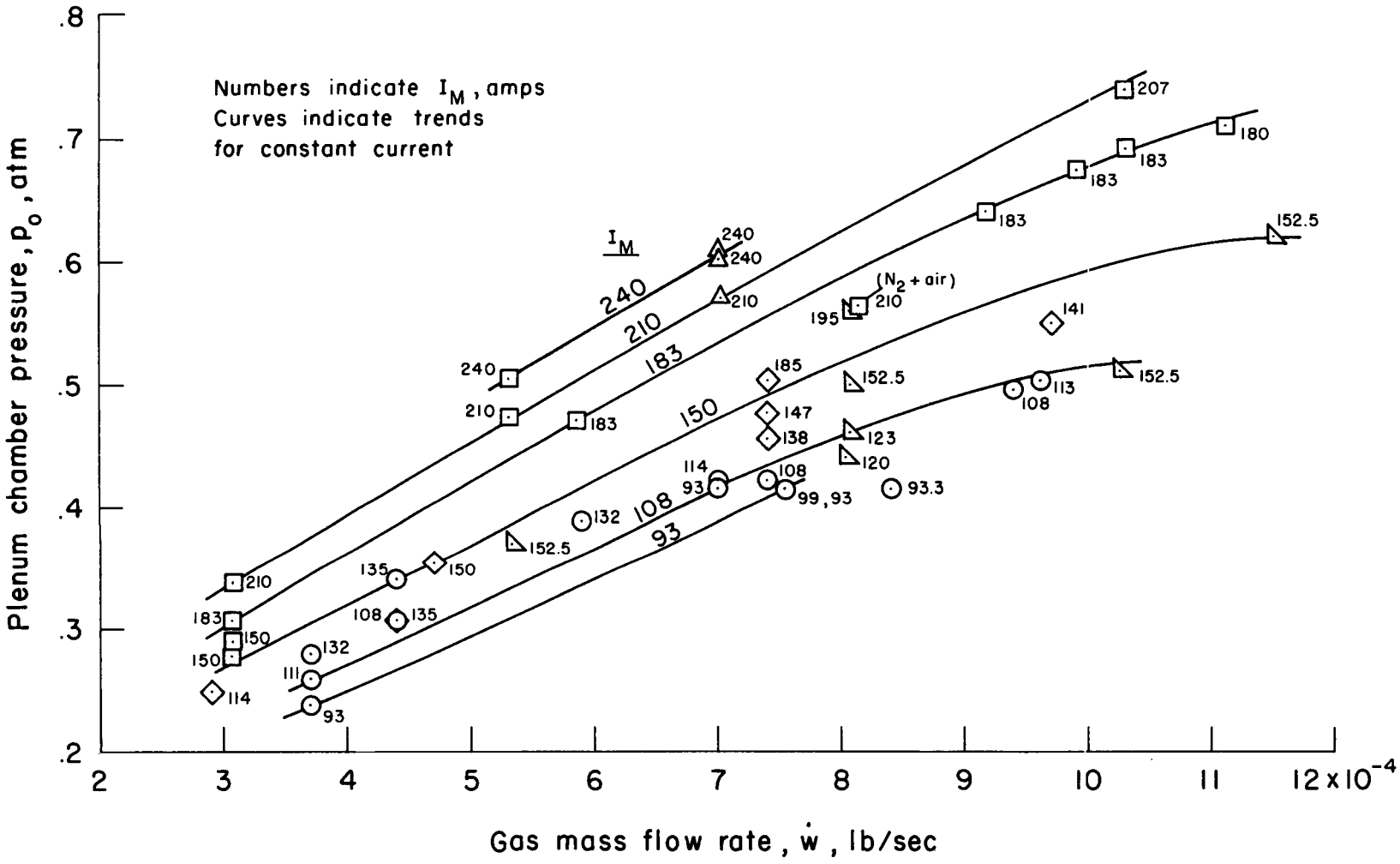

Figure 13.- Plenum chamber pressure as a function of nitrogen flow rate and arc current.

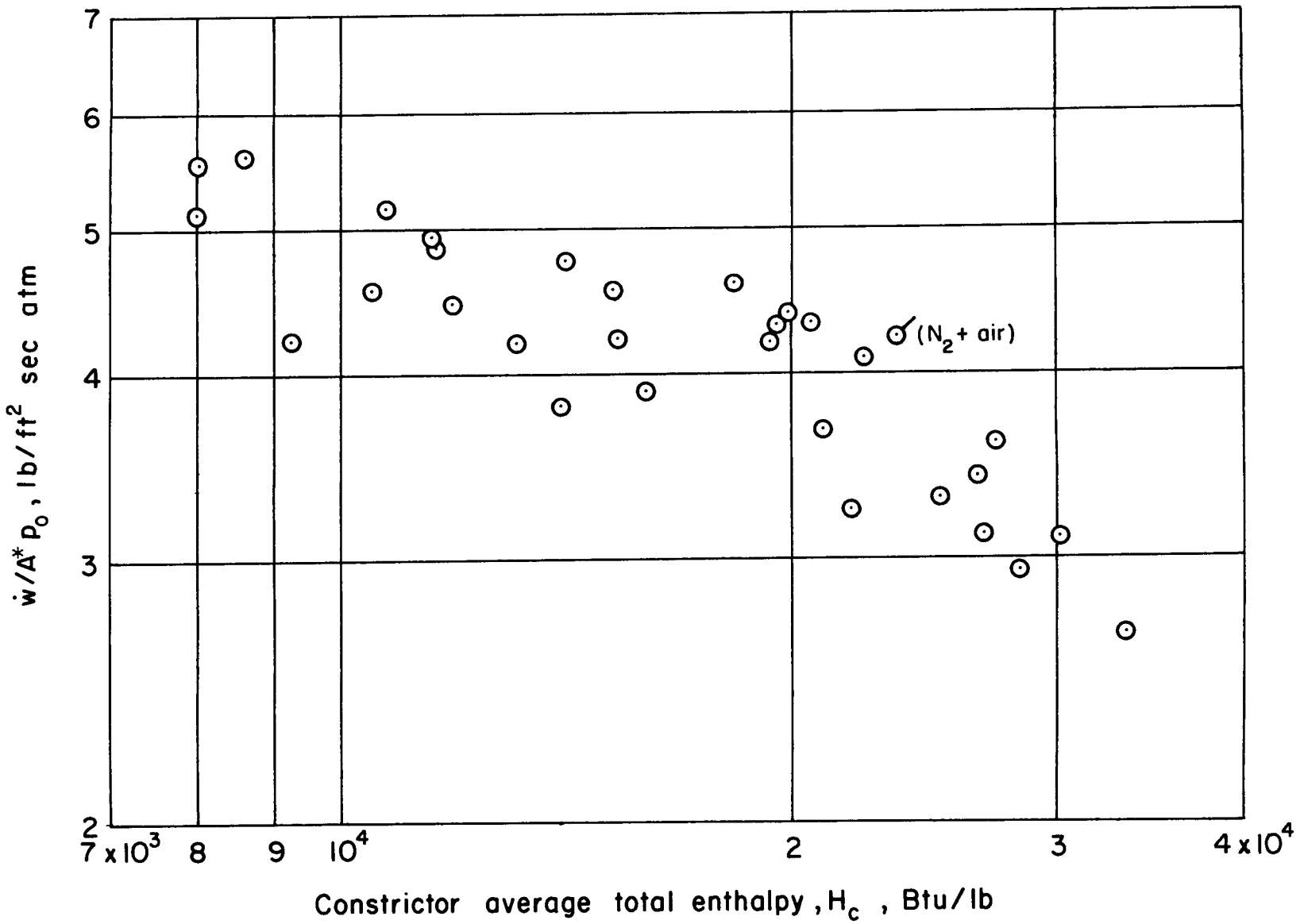

Figure 14.- Critical flow parameter, $\dot{w}/A^* p_o$ as a function of stagnation enthalpy at downstream end of constrictor.

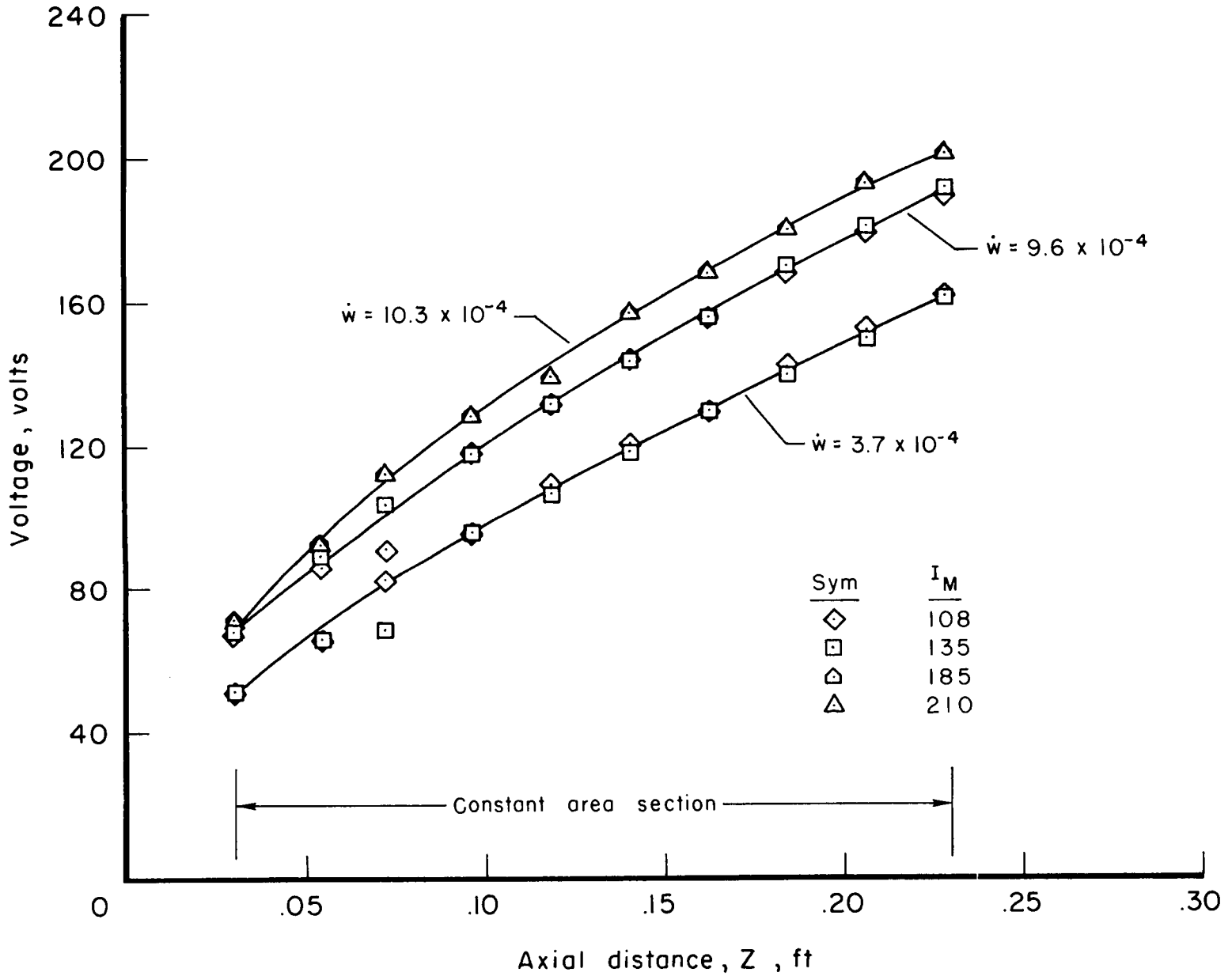

Figure 15.- Voltage as a function of axial distance for various arc currents and nitrogen flow rates.

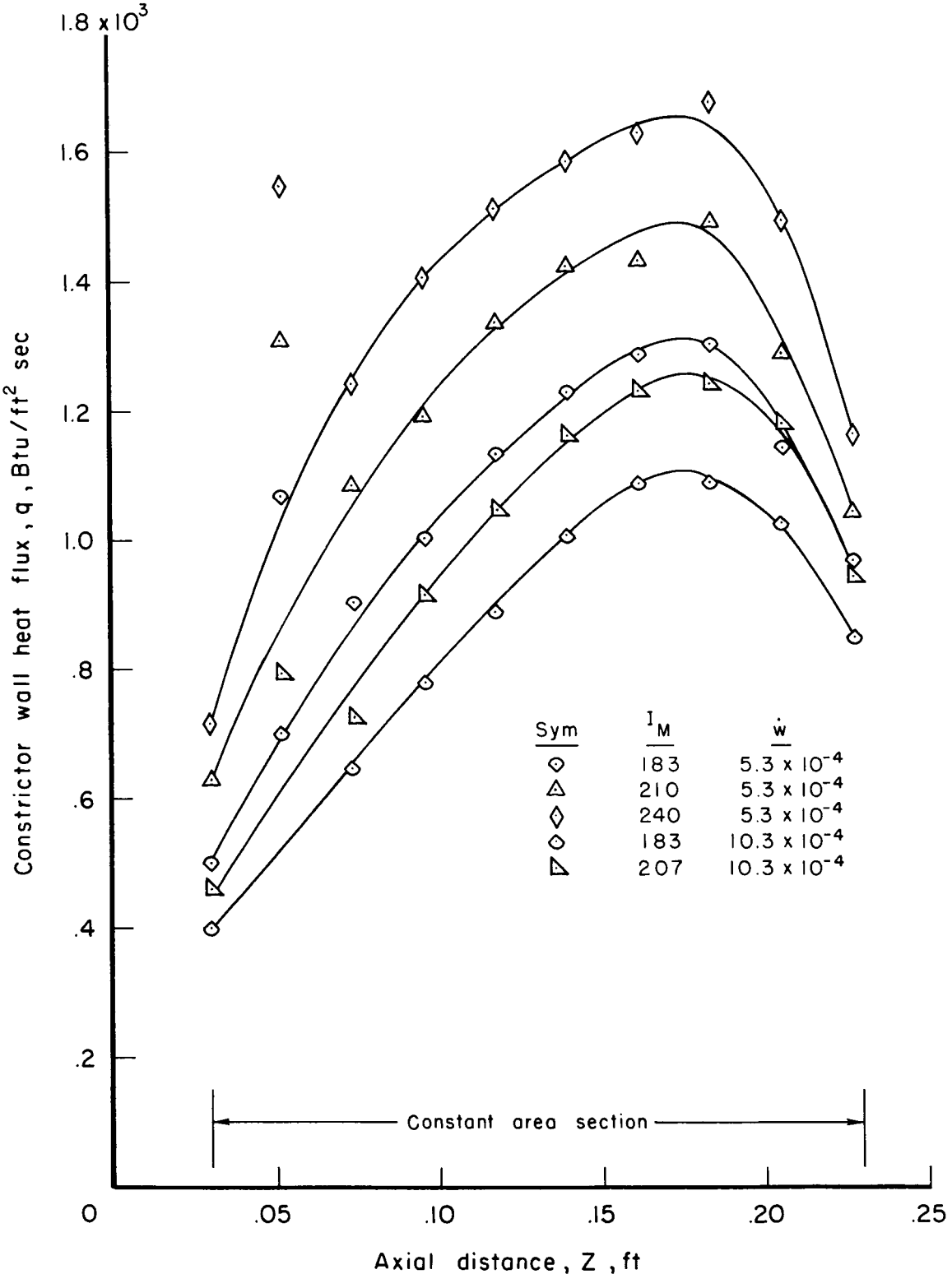

Figure 16.- Constrictor wall heat flux versus axial distance for various arc currents and nitrogen flow rates.

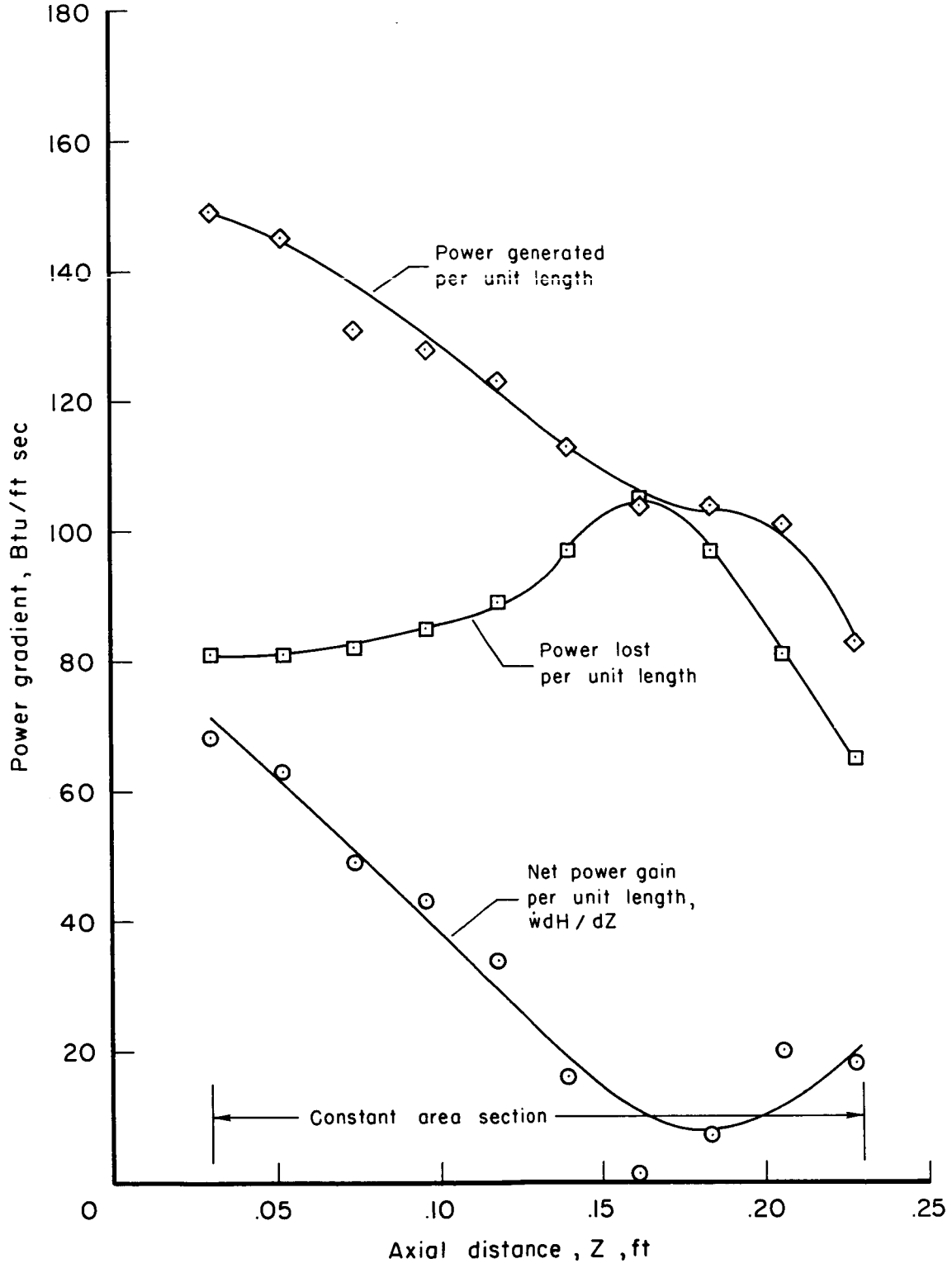

Figure 17.- Constrictor power gradient versus axial position I_M = 210 amp, nitrogen flow rate = 5.3×10^{-4} lb/sec.

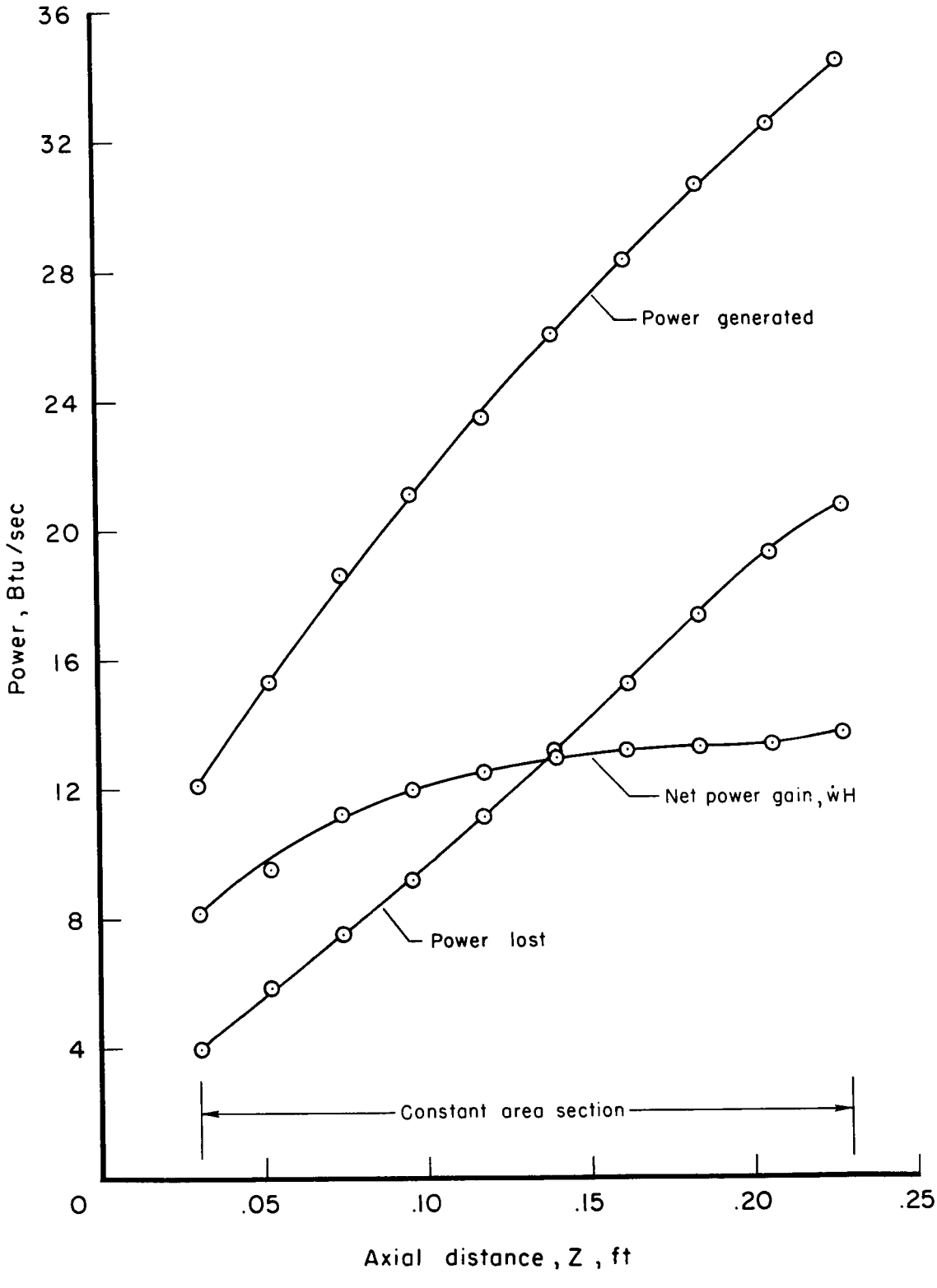

Figure 18.- Constrictor power versus axial position; I_M = 210 amp, nitrogen flow rate = 5.3×10^{-4} lb/sec.

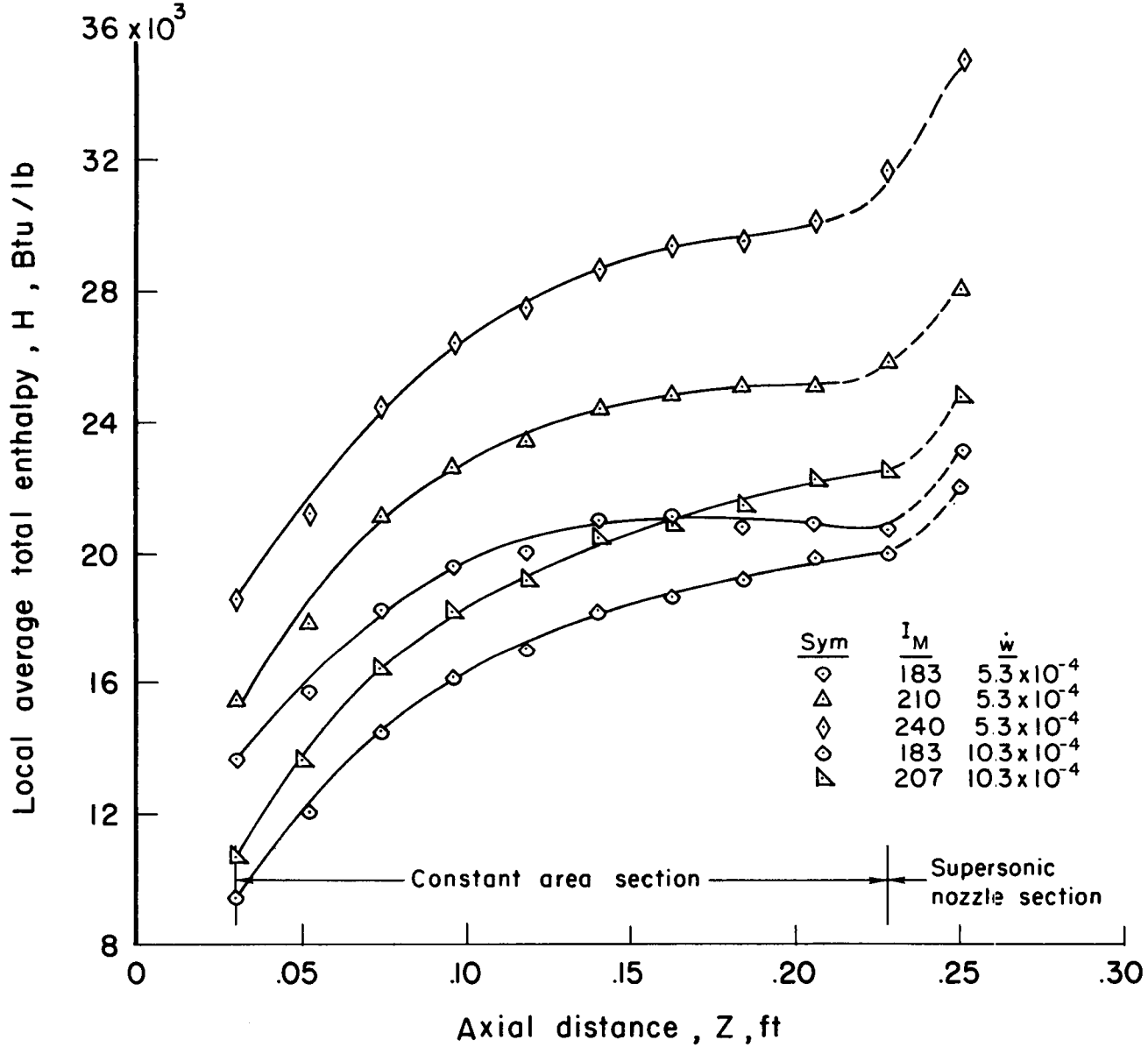

Figure 19.- Constrictor average total enthalpy versus axial distance for various arc currents and nitrogen flow rates.

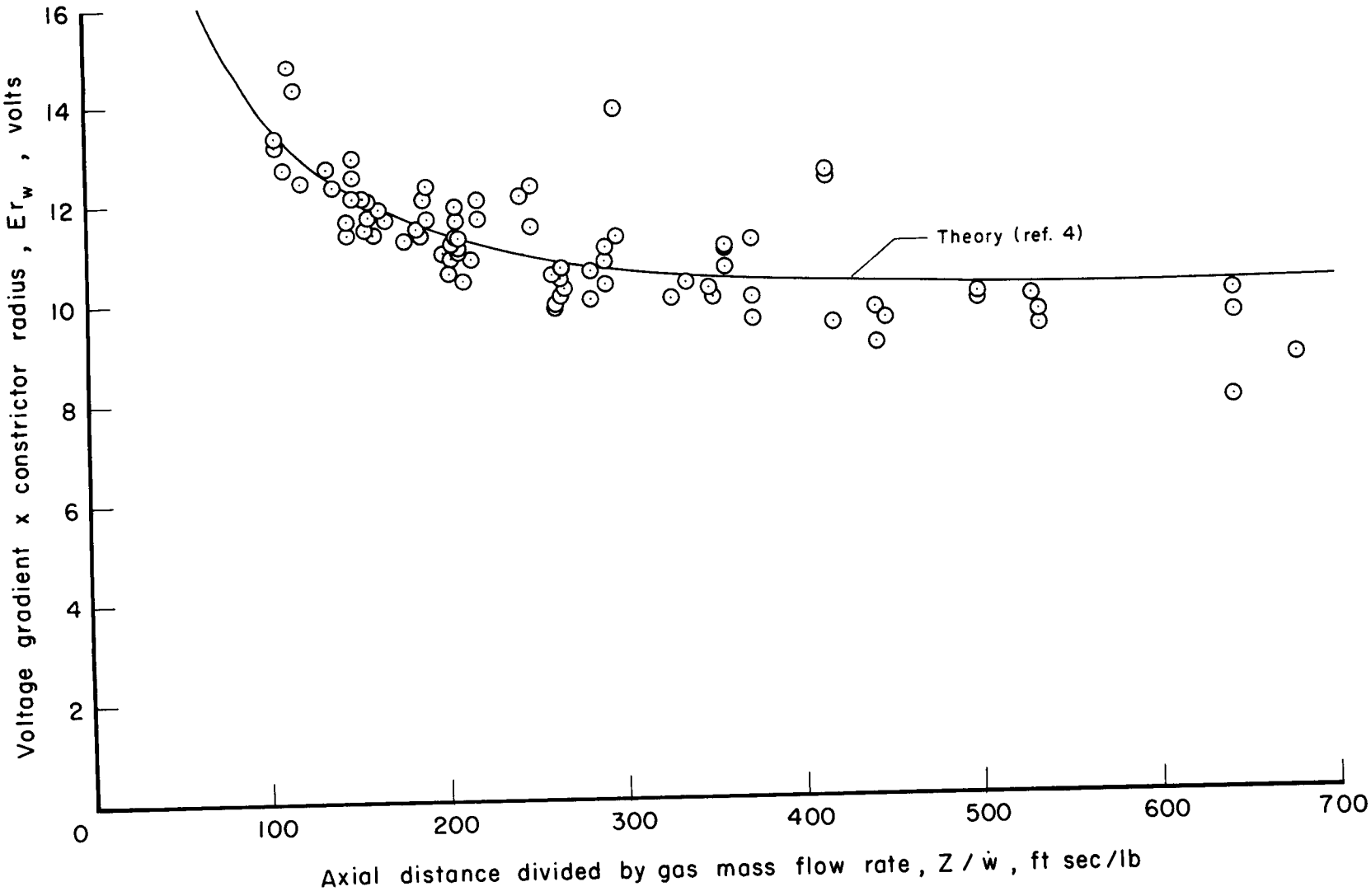

Figure 20.- Variation of voltage parameter with ratio of length to flow rate.

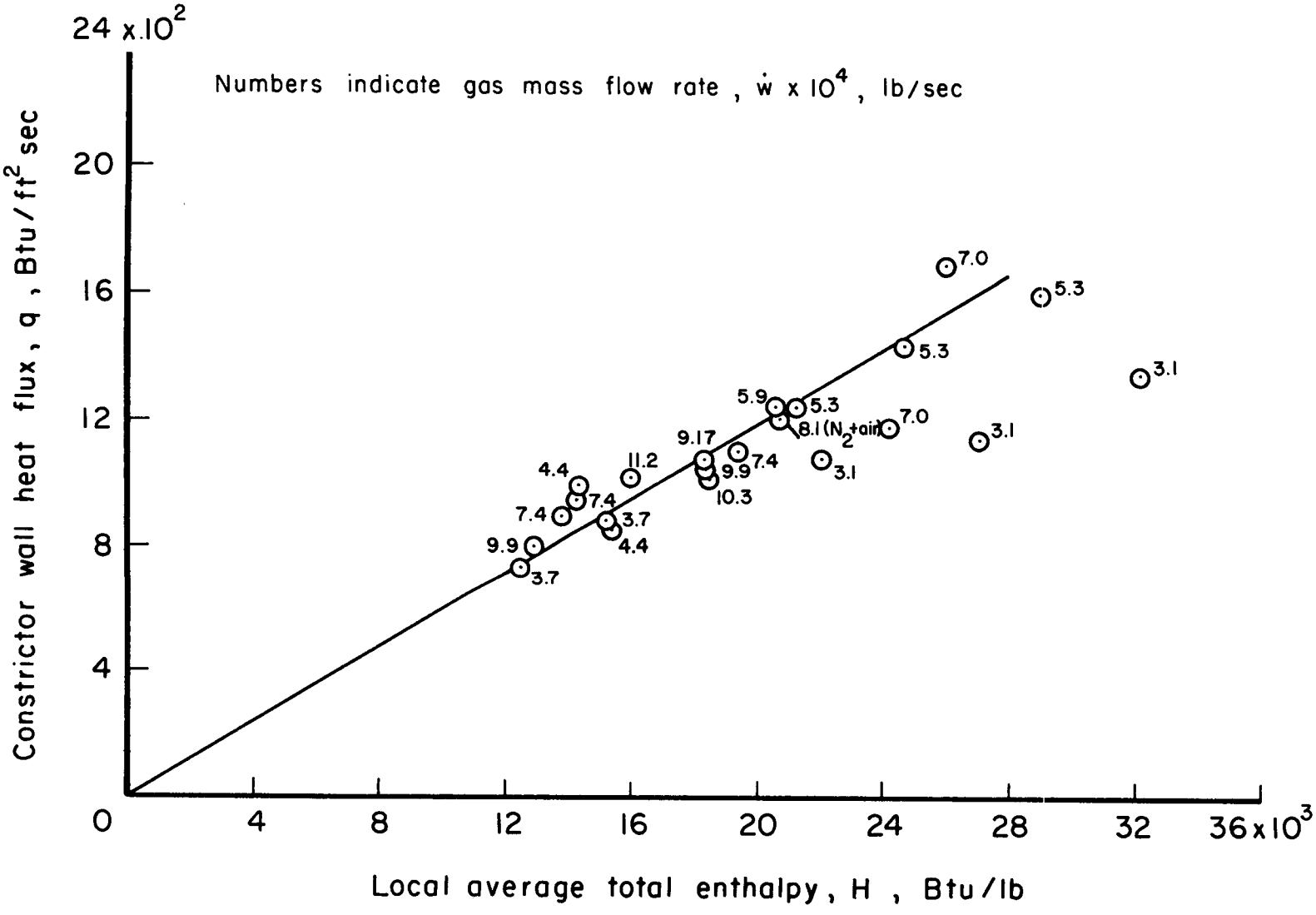

Figure 21.- Variation of constrictor wall heat flux with local average total enthalpy for various nitrogen flow rates; Z = 0.14 ft.

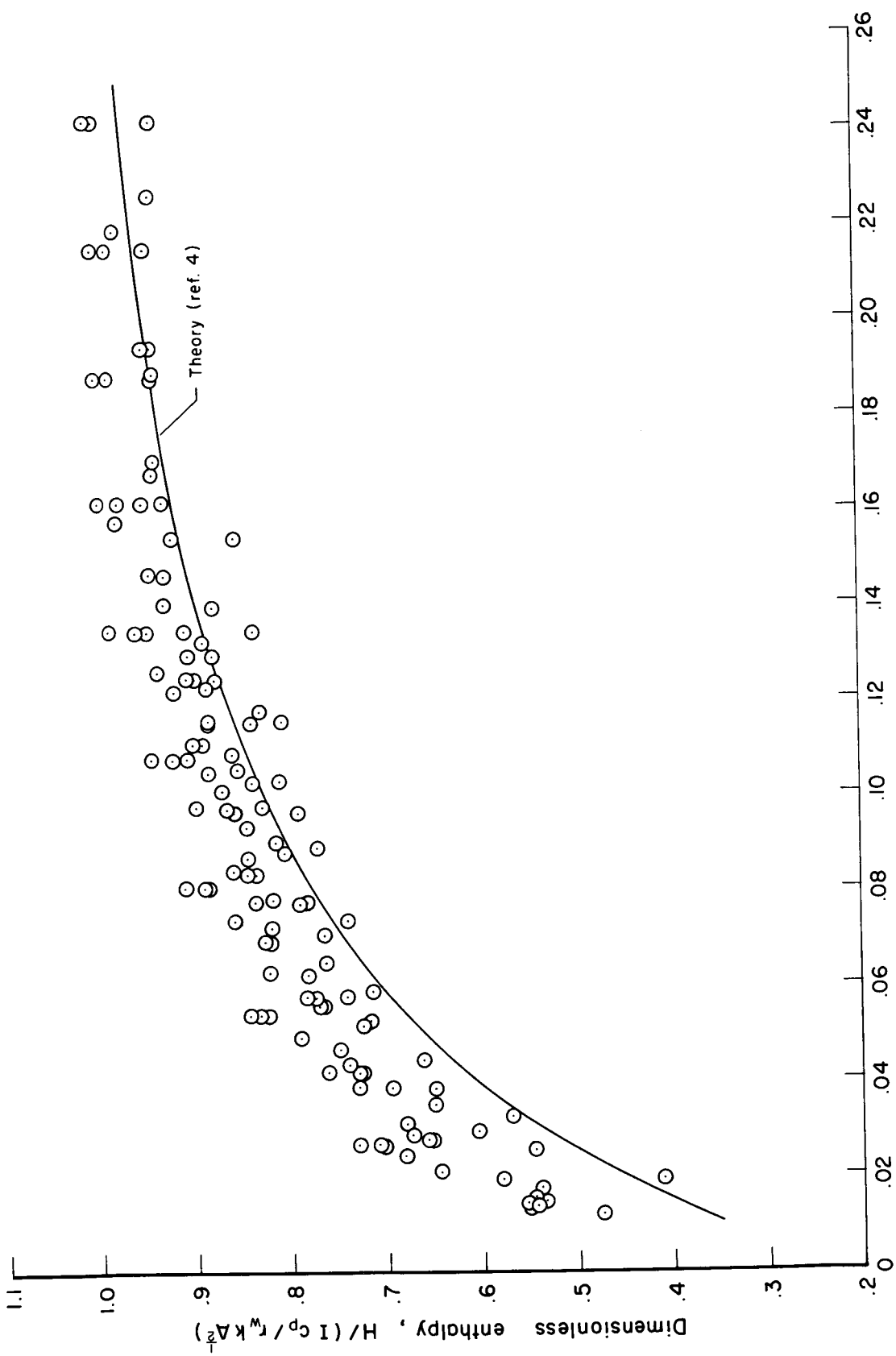

Figure 22.- Variation of normalized enthalpy distribution with normalized length.

NASA-Langley, 1964 A-744